

January 2011

Characterization Of Pregnancy Induced Cardiac Hypertrophy In Rats

Patricia Holden
Eastern Kentucky University

Follow this and additional works at: <https://encompass.eku.edu/etd>



Part of the [Molecular Biology Commons](#)

Recommended Citation

Holden, Patricia, "Characterization Of Pregnancy Induced Cardiac Hypertrophy In Rats" (2011). *Online Theses and Dissertations*. 35.
<https://encompass.eku.edu/etd/35>

This Open Access Thesis is brought to you for free and open access by the Student Scholarship at Encompass. It has been accepted for inclusion in Online Theses and Dissertations by an authorized administrator of Encompass. For more information, please contact Linda.Sizemore@eku.edu.

Characterization of Pregnancy Induced Cardiac Hypertrophy in Rats

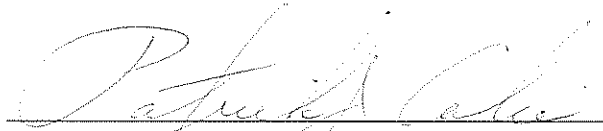
By:

Patricia Holden

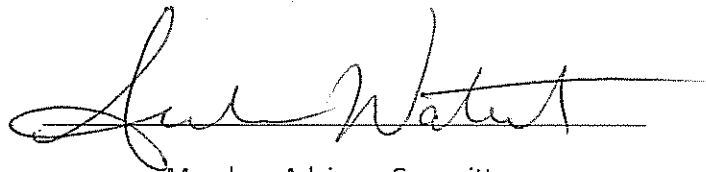
Thesis Approved:

A handwritten signature in cursive script, reading "Rebekah Wainel", written over a horizontal line.

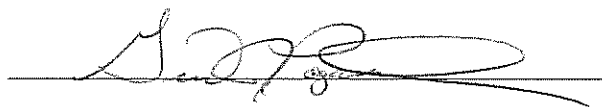
Chair, Advisory Committee

A handwritten signature in cursive script, reading "Patricia Cole", written over a horizontal line.

Member, Advisory Committee

A handwritten signature in cursive script, reading "Lee Watson", written over a horizontal line.

Member, Advisory Committee

A handwritten signature in cursive script, written over a horizontal line.

Dean, Graduate School

STATEMENT OF PERMISSION TO USE

In presenting this thesis in partial fulfillment of the requirements for a Master's degree at Eastern Kentucky University, I agree that the Library shall make it available to borrowers under the rules of the Library. Brief quotations from this thesis are allowable without special permission, provided that accurate acknowledgement of the source is made.

Permission for extensive quotation from or reproduction of this thesis may be granted by my major professor, or in her absence, by the Head of Interlibrary Services when, in the opinion of either, the proposed use of the material is for scholarly purposes. Any copying or use of the material in this thesis for financial gain shall not be allowed without my written permission.

Signature *Pain Holden*

Date 5-23-11

CHARACTERIZATION OF PREGNANCY INDUCED CARDIAC HYPERTROPHY
IN RATS

By
PATRICIA I. HOLDEN

Bachelor of Science
Ohio University
Athens, Ohio
2009

Submitted to the Faculty of the Graduate School of
Eastern Kentucky University
in partial fulfillment of the requirements
for the degree
MASTER OF SCIENCE
August, 2011

Copyright © Patricia Holden, 2011
All rights reserved

Acknowledgments

I would first like to thank Dr. Rebekah Waikel for her support, guidance, and encouragement throughout the past several years. Thanks to my committee members, Dr. Pat Calie and Dr. Amanda Waterstrat for all of their help during my thesis project and writing. This work was made possible through the University Research Committee grant at Eastern Kentucky University.

Characterization of Pregnancy Induced Cardiac Remodeling in Rats

During pregnancy, an increase in blood volume occurs to compensate for fetal development, resulting in cardiac hypertrophy. For the majority of women, this physiological cardiac hypertrophy resolves following pregnancy. Prolonged cardiac hypertrophy can lead to heart failure. We propose that by studying the biochemical mechanisms that mediate healthy cardiac remodeling associated with pregnancy, we will gain a better understanding of mechanisms involved in pathological cardiac hypertrophy. To determine the biochemical changes that occur during pregnancy induced cardiac remodeling, we subjected rats to timed matings and collected morphological and biochemical data from not pregnant, 19 days pregnant, and 24 hours postpartum. The heart weights increased approximately 6% on the 19th day of pregnancy as compared to their non-pregnant littermates. Histological analysis confirmed an increase in cardiomyocyte size associated with the increase in heart size. Real-time PCR analysis revealed alterations in expression of some gene markers of hypertrophy during pregnancy and postpartum. Our data demonstrates pregnancy induced cardiac remodeling in the rat involves both morphological and biochemical changes.

TABLE OF CONTENTS

CHAPTER	
I.	INTRODUCTION1
II.	MATERIALS AND METHODS.....29
III.	SPECIFIC AIM 1: Morphological Characterization of Pregnancy Induced Cardiac Hypertrophy and Post-Partum Cardiac Remodeling36
IV.	SPECIFIC AIM 2: Biochemical Characterization of Pregnancy Induced Cardiac Hypertrophy and Post-Partum Cardiac Remodeling.....44
V.	SPECIFIC AIM 3: MiRNA signature of Pregnancy Induced Hypertrophy and Post-Partum Resolution48
VI.	SUMMARY AND FUTURE DIRECTIONS52
	REFERENCES55
	APPENDIXES62
	A. IACUC Approval Letter62
	B. Dr. Rebekah Waikel’s FastPrep RNA Extraction Protocol64
	C. Individual Cardiomyocyte Areas67

LIST OF FIGURES

Figure

1. Pathological and physiological hypertrophy in the mouse model	2
2. Cellular signaling mechanisms of both estrogen receptors.....	7
3. Schematic of the gene expression markers of hypertrophy	10
4. Processing of the natriuretic peptides	13
5. Schematic of miRNA activation	17
6. Phylogenic relationship between three species.....	27
7. Heart to body weight ratios for each group	37
8. Heart weight (mg) to tibia length (mm) ratios for each group.....	38
9. Cardiomyocyte areas for each group	39
10. H&E stained 5 μ m cross section samples for each group.....	40
11. Expression levels for each α -MHC, GPER, ANP and BNP	45
12. Expression levels for miR-1, miR-133a, miR-21 and miR-195	49

LIST OF TABLES

Table

1. Differences between physiological and pathological cardiac hypertrophy	4
2. miRNA expression profiles for miR-1, miR-133a, miR-195 and miR-21 assembled through a literature review	20
3. Primer sets utilized for Gene Expression Real Time PCR	32
4. Primer sets utilized for miRNA Real Time PCR	34
5. Individual cardiomyocyte areas measured in μm^2	68

Chapter 1

Introduction

Objective

While pathologic cardiac hypertrophy has been well characterized, little analysis has been conducted on pregnancy induced cardiac hypertrophy (van Rooij *et al.*, 2008; Eghbali *et al.*, 2005). This study was undertaken to provide a) morphological and biochemical data in an attempt to correlate pregnancy induced cardiac hypertrophy with pathological cardiac hypertrophy; and b) to provide a detailed miRNA and gene expression characterization during pregnancy induced cardiac remodeling was also completed. Together these data could potentially distinguish whether pregnancy induced cardiac hypertrophy could be used as a model to study and treat pathological cardiac hypertrophy.

Cardiac Hypertrophy and Heart Failure

Cardiac hypertrophy is defined as “an increase in cardiomyocyte size that can be beneficial and adaptive (physiological) or maladaptive (pathological) phenomenon to compensate for the hemodynamic stress resulting from pressure or volume overloads (Eghbali *et al.*, 2005).” In response to a chronic increase in cardiac load such as either chronic exercise or pregnancy, there is an initial increase in heart mass to normalize the wall stress (Bernardo *et al.*, 2010). If the chronic increase in wall stress is not relieved, the hypertrophied heart can dilate, all contractive function fails, and in response, the heart fails (Bernardo *et al.*, 2010; Yue *et al.*, 2000). Hypertrophy often leads to heart failure in humans and is a major determinant of mortality and morbidity in cardiovascular diseases (Zhang, 2008). Heart failure is considered to be one of the most frequent causes of death in industrialized countries (Ahmad *et al.*, 2005; Buitrago *et al.*, 2005). Currently there is no cure for heart failure. Long term survival remains poor as one third of patients typically die in the first year of their diagnosis (Bernardo *et al.*, 2010). This emerging epidemic costs more than \$17 billion annually in health care costs (Ahmad *et al.*, 2005).

The cardiac muscle is composed of many myocytes, which are in turn composed of myofibrils. The myocytes are arranged around the left ventricle and contract with the heart to maintain a steady beating pace. The myofibrils are made of sarcomeres, the basic contractile unit of the heart and most muscles. Hypertrophy is considered a cellular response that shows an increase in protein synthesis and disarray in sarcomere assembly (Buitrago *et al.*, 2005). A schematic of cardiac hypertrophy can be found in Figure 1. Intercalated discs, located at the ends of the myocytes, are responsible for maintaining cell to cell adhesion while allowing contractile forces to be transmitted through the cells (Bernardo *et al.*, 2010). Myocytes have an intrinsic mechano-sensing mechanism, as stretch sensitive ion channels present in the plasma membrane play a link in coordinating the extracellular matrix, cytoskeleton, sarcomere, calcium handling proteins and nucleus (Bernardo *et al.*, 2010).

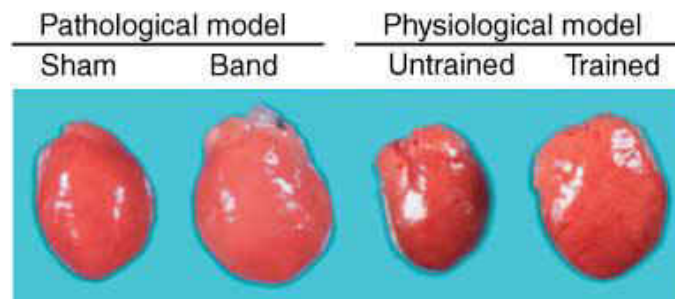


Figure 1. Pathological and Physiological hypertrophy in the mouse model. In the pathological model, the mouse had aortic banding for one week, shown on the right, as compared to their Sham littermates. In the physiological model, mice were subject to chronic swim training for 4 weeks. Although pathological and physiological cardiac hypertrophy result from different stimuli, both pathological and physiological result in an enlargement of the heart.

Source: McMullen, J.R. and Jennings, G.L. (2007). Differences between pathological and physiological cardiac hypertrophy: novel therapeutic strategies to treat heart failure. *Clin. Exp. Pharmacol. Physiol.*, 34, 255-262.

Molecular techniques have enabled researchers to determine the degree of hypertrophy. Genes that have been studied in mouse include: α -MHC, β -MHC, ANP and BNP (Eghbali *et al.*, 2005). Other methods in the laboratory include echocardiograms to determine the thickness of the ventricular wall, and weighing the mass of the heart and body of the animal (Eghbali *et al.*, 2005, Virgen-Ortiz *et al.*, 2009). It has been reported

that during cardiac hypertrophy there is around a 15% increase in heart-to-body weight ratio (Virgen-Ortiz *et al.*, 2009). In early hypertrophic studies in animals with aortic banding, the left ventricle weight (LVW) relative to body weight increased 65% compared to the sham (control) group after 14 days (Busk & Cirera, 2010). A recent technique to determine hypertrophy in mice is utilizing the heart weight when comparing to the tibia length (Seixas Bello Moreira *et al.*, 2009).

Scientists aim to utilize many of these techniques in a clinical diagnostic setting. Currently, the standard in a clinical setting is use of an echocardiogram for left ventricular thickness. Through rapid identification of hypertrophy, therapeutic options could become available to assist in a healthy remodeling process, including administration of peptides that inhibit hypertrophy.

Pathological and Physiological Cardiac Hypertrophy

Cardiac hypertrophy can be classified as a pathological and physiological response. Physiological cardiac hypertrophy is a result of pregnancy and excessive exercise especially during training, pathological hypertrophy is a result of hypertension, valvular insufficiency, endocrine disorders and genetic mutations (Catalucci *et al.*, 2008, McMullen & Jennings, 2007). Despite the comparable increases in heart size, as shown in Figure 1, pathological and physiological hypertrophy are associated with distinct structural, functional, metabolic, biochemical and molecular features, as mentioned in Table 1 (Bernardo *et al.*, 2010).

Table 1. Differences between physiological and pathological cardiac hypertrophy. Both pathological and physiological hypertrophy result in increased myocyte volume and formation of new sarcomeres. Pathological hypertrophy, however, usually results in heart failure, while physiological cardiac hypertrophy does not.

	Pathological cardiac hypertrophy	Physiological cardiac hypertrophy
Stimuli	Pressure load in a disease setting (e.g. hypertension, aortic coarctation) or volume load (e.g. valvular disease) Cardiomyopathy (familial, viral, toxic, metabolic)	Regular physical activity or chronic exercise training Volume load (e.g. running, walking, swimming) Pressure load (e.g. strength training, weight lifting)
Cardiac morphology	Increased myocyte volume Formation of new sarcomeres Interstitial fibrosis Myocyte necrosis and apoptosis	Increased myocyte volume Formation of new sarcomeres
Fetal gene expression	Usually upregulated*	Relatively normal*
Cardiac function	Depressed over time	Normal or enhanced
Completely reversible	Not usually	Usually
Association with heart failure and increased mortality	Yes	No

*Biological significance not clear.

Source: McMullen, J.R. and Jennings, G.L. (2007). Differences between pathological and physiological cardiac hypertrophy: novel therapeutic strategies to treat heart failure. *Clin. Exp. Pharmacol. Physiol.*, 34, 255-262.

Physiological and pathological hypertrophy can be further distinguished into two specific areas of hypertrophy, concentric and eccentric. As the heart experiences pathological hypertrophy and pressure overload, the systolic wall stress then results in concentric hypertrophy; distinguishable by thick walls and small cavities (McMullen & Jennings, 2007). On a cellular level the cardiac myocytes enlarge and form new sarcomeric structures, intended to normalize wall stress and prevent normal cardiovascular function during resting periods (McMullen & Jennings, 2007). As a result of the cardiovascular function decompensating, the chambers remain a normal size and the left ventricle dilates, thus resulting in heart failure (McMullen & Jennings, 2007). Pathological hypertrophy is associated with cell death and the loss of myocytes that are replaced with excess collagen (Bernardo *et al.*, 2010). Excessive collagen stiffens the ventricles, thus impairing contraction and relaxation (Bernardo *et al.*, 2010). The electrical coupling of cardiac myocytes is extracellular matrix proteins that also reduce capillary density (Bernardo *et al.*, 2010). During periods of volume overload in pathological hypertrophy, aortic regurgitation causes an increase in diastolic wall stress and results in eccentric hypertrophy (McMullen & Jennings, 2007). Eccentric

hypertrophy, often seen in physiological hypertrophy results in chamber enlargement, considered to be a proportional change to the left ventricular wall thickness (McMullen & Jennings, 2007). Eccentric hypertrophy often enhances cardiac function in resting conditions to help satisfy the increased cardiac demands placed on the body (Iemitsu *et al.*, 2005). The main difference between eccentric and concentric hypertrophy is that during eccentric hypertrophy, the heart does not decompensate into dilated cardiomyopathy or result in heart failure (McMullen & Jennings, 2007).

Although a strong determinant of hypertrophy is blood pressure, interactions between many genes and the environment are likely to contribute to the development of hypertrophy (Barrick *et al.*, 2009). The cellular mechanisms behind both concentric and eccentric cardiac hypertrophy are now understood. Generally, the $G_{\alpha q}$ pathway regulates pathological hypertrophy while the Insulin Growth Factor 1 Phosphoinositide-3 kinase (IGF1-PI3K) pathway regulates physiological hypertrophy (McMullen & Jennings, 2007).

Pathological cardiac hypertrophy generally results in concentric hypertrophy, which is tightly regulated by the $G_{\alpha q}$ pathway (McMullen & Jennings, 2007). The $G_{\alpha q}$ pathway is initially activated by angiotensin II (Ang II), endothelin 1 (ET-1) and noradrenaline (McMullen & Jennings, 2007). Once activated, a G-Protein Coupled Receptor (GPCR) is also activated and leads to the disassociation of $G_{\alpha q}$ and activation of downstream molecules. Using a transgenic mouse model and over-expression of the Ang II receptor along with a peptide that inhibits $G_{\alpha q}$, the coupled receptor signaling did not develop hypertrophy, supporting the hypothesis that $G_{\alpha q}$ is responsible for pathological hypertrophy (McMullen & Jennings, 2007).

Physiological cardiac hypertrophy results in eccentric hypertrophy and is regulated by the IGF1-PI3K pathway (McMullen & Jennings, 2007). In the IGF1-PI3K pathway, IGF1 acts via the IGF-Receptor (IGFR) to initiate a tyrosine kinase, which then activates PI3K (McMullen & Jennings, 2007). PI3K then releases inositol lipid products from the plasma membrane that mediate intracellular signaling (McMullen & Jennings, 2007). When transgenic mice with enhanced IGF1-PI3K signaling developed

hypertrophy, their life span was normal and cardiac function was normal or even enhanced (McMullen & Jennings, 2007). Mice expressing lower cardiac IGF1-PI3K signaling had smaller hearts, suggesting that P13K pathway is crucial in the physiological growth of the heart (McMullen & Jennings, 2007).

Other proteins that regulate cardiac hypertrophy include Rho, GSK-3 β and NGFIA. Rho contributes to various cellular functions such as actin cytoskeleton organization, cell adhesion and cytokinesis (Balakumar & Singh, 2006). Rho is also suggested to be involved in mechanical stress induced cardiac hypertrophy in cardiac myocytes as well as left ventricular remodeling (Balakumar & Singh, 2006). Rho mediates the up-regulation of pro-inflammatory cytokines, reactive oxygen species and transforming growth factor β (Balakumar & Singh, 2006). GSK-3 β is constitutively expressed on active serine and/or threonine kinase residues that phosphorylate cellular substrates (Iemitsu *et al.*, 2005). GSK-3 β also regulates a variety of cellular functions, including: metabolism, gene transcription, cell cycle regulation and apoptosis; it is also a negative regulator of cardiomyocyte hypertrophy (Iemitsu *et al.*, 2005). NGFIA binding protein (Nab1) is a member of a co-receptor family (Buitrago *et al.*, 2005). Nab1 is an active repressor that interferes directly with the general transcription process (Buitrago *et al.*, 2005). Nab1 does not affect physiological hypertrophy; however, the connection to pathological hypertrophy has not yet been established.

Estrogen

Estrogen is considered the most important hormone in the woman's body because it plays a role in the reproductive, immune, vascular and nervous systems (Prossnitz & Barton, 2009). Estrogen can be found in not only natural sources such as phytoestrogens and soybased products and, in synthetic forms including xenoestrogens, pesticides, herbicides, polychlorinated biphenyl and plasticizers (Prossnitz & Barton., 2009).

Prior studies have determined the development of exercise mediated cardiac hypertrophy in a sex specific manner. Female mice typically exhibit an increased cardiac hypertrophic response in treadmill protocols as compared to the male mice. Females also show an increased exercise capacity when compared to male mice (Foryst-Ludwig *et al.*,

2011, Pedram *et al.*, 2008). The underlying mechanisms of sex specific differences during cardiac hypertrophy are yet to be understood (Foryst-Ludwig *et al.*, 2011).

Estrogen Receptors: ER- α , ER- β and GPER

Estrogen is predominantly synthesized in the ovaries. After synthesis, it passes through cell membranes by simple diffusion (Prossnitz & Barton., 2009). The physiological response to estrogen is initiated by cellular receptors, as shown in Figure 2 (Dennis *et al.*, 2009). This binding results in altered protein on protein interactions and activation of several cellular signaling pathways, as shown in Figure 2 (Dennis *et al.*, 2009).

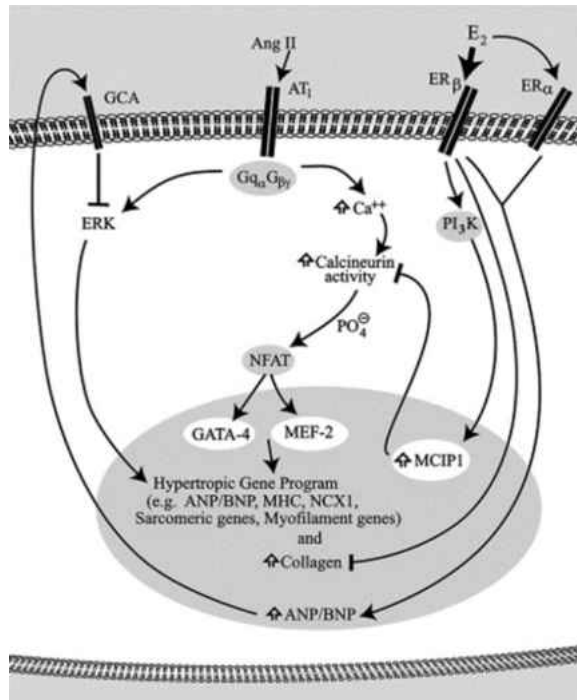


Figure 2. Cellular signaling mechanisms of both estrogen receptors. The Gq_s turns on the ERK pathway, which in turn activates the hypertrophic gene program. The PI3K pathway is activated through the estrogen receptors, which upregulates MCIP1, that inhibits calcineurin activity.

Source: Pedram, A., Razandi, M., Lubahn, D., Liu, J., Vannan, M. and Levin, E.R. (2008). Estrogen inhibits cardiac hypertrophy: role of estrogen receptor- β to inhibit calcineurin. *Endocrinology*, 149, 3361-3369.

The rapid response of estrogen is highly associated with the cell surface receptors including growth factor receptors and G-Protein Coupled Receptors. The two highly studied estrogen receptors, also referred to as the classic estrogen receptors, include Estrogen Receptor α (ER- α) and Estrogen Receptor β (ER- β) (Prossnitz & Barton, 2009). These estrogen receptors function traditionally as ligand-activated nuclear transcription factors that bind to the regulatory response elements in the promoters of genes (Prossnitz & Barton, 2009).

For several years, ER- α and ER- β were the only two classic estrogen receptors. Subsequently, a 7 trans-membrane G protein coupled receptor, also known as GPR30 or GPER, was identified to activate similar cellular signaling pathways as ER- α and ER- β (Dennis *et al.*, 2009). GPER can mediate estrogen induced non-genomic signaling events, including stimulation of adenylyl cyclase, transactivation of epidermal growth factor receptors, activation of the mitogen activated protein kinase (MAPK) and the phosphatidylinositol 3 kinase (PI3K) pathways (Ariazi *et al.*, 2010). The gene for human GPER is located on chromosome 7p22.3 and is composed of three exons (Mizukami, 2010). Based on linkage analysis, the chromosomal region containing GPER is thought to be related to familial hypertensive disease in humans (Mizukami, 2010).

Studies have further emphasized that estrogen is capable of binding to and activating the classic estrogen receptors as well as GPER; thus indicating that there is a lack of specificity between the three receptors (Prossnitz & Barton, 2009). In fact, ER- α and ER- β appear to overlap with GPER not only in cellular and physiological responses, but also in ligand specificity (Dennis *et al.*, 2009).

Scientists have begun to utilize GPER agonists and antagonists such as G-1 and G-15, in order to study the cellular and physiological effects of GPER. An agonist is a chemical substance capable of activating a receptor to induce a full or partial pharmacological response; while an antagonist is a substance utilized that counteracts the effects of other substances (Dennis *et al.*, 2009). The G-1 agonist shows no detectable activity towards the classic estrogen receptors (Dennis *et al.*, 2009). G-1 has been able to probe the role of GPER *in vivo* with reported effects including experimental autoimmune

encephalomyelitis (Dennis *et al.*, 2009). Other findings indicate that G-1 activated GPER blocks cell cycle progression at the G1 phase, indicating a potential cancer target (Ariazi *et al.*, 2010). G-1 also mediates protection by activating acute signaling pathways, including the P13K pathway (Deschamps & Murphy, 2009). The G-15 antagonist was initially chemically synthesized by Dennis *et al.* in 2009, was able to inhibit cellular signaling as well as GPER mediated functions *in vivo*. Through utilizing similar techniques, Ariazi *et al.* was able to identify that GPER, not ER α , mediates the estrogen receptor induced calcium mobilization response (Ariazi *et al.*, 2010). Utilizing agonists such as G-1 and antagonists such as G-15 are the very beginnings of finding specific therapeutic targets for diseases in the GPER receptor pathways, such as cancer and other endocrine disorders.

The Role of Estrogen in Cardiac Hypertrophy

For many years estrogen was considered a cardioprotective agent, as pre-menopausal women have a decreased risk of cardiovascular disease relative to males (Deschamps & Murphy, 2009). These numbers shift; however, in post-menopausal women, as the risk of developing a cardiovascular disease reaches or even exceeds that of men (Deschamps & Murphy, 2009). In fact, heart failure from cardiovascular disease remains the number one killer in women today (Pedram *et al.*, 2008).

Animal studies have supported the anti-hypertrophic effects of estrogen in the heart (Pedram *et al.*, 2008). Estrogen supplementation of ovariectomized female mice causes a 30% reduction in pressure overload-induced hypertrophy (Pedram *et al.*, 2008). Pedram *et al.* conducted a study in 2008 to determine the role that estrogen plays during TAC induced cardiac hypertrophy. This study concluded many significant findings: First, estrogen inhibits cardiac hypertrophy through ER β receptor in order to counteract the effects of the peptide AngII (Pedram *et al.*, 2008). Ang II then activates several pathways to initiate hypertrophy (Pedram *et al.*, 2008).

Recently, two clinical trials designed to test the effects of estrogen replacement in postmenopausal women, the Women's Health Initiative (WHI) and the Heart and Estrogen/Progestin Replacement Study (HERS) found that estrogen did not reverse

cardioprotective effects and actually increased the number of cardiovascular events (Deschamps & Murphy, 2009). Previous to these studies, estrogen has been identified as a cardioprotective agent, especially for females. It is now even more important to understand the mechanisms by which estrogen exerts its protective effects on the heart (Deschamps & Murphy, 2009).

Genetic Markers of Hypertrophy

Genetic markers of pathological hypertrophy have been well known for many years. For example, the heart reacts to cardiac injury by activating a range of signaling pathways by switching the pattern of expressed genes to an embryonic profile (Zorio *et al.*, 2009). These embryonic expression patterns are seen in Figure 3. Pathological cardiac hypertrophy is associated with direct alterations in cardiac contractile proteins, such as: α and β myosin heavy chains, increased levels of natriuretic peptides atrial natriuretic peptide (ANP) and brain natriuretic peptide (BNP), and lastly, down-regulation of calcium handling proteins, such as SERCA2a (Bernardo *et al.*, 2010). In a recent study done in a mouse model, physiological studies did not show any significant change in any of these genes (Iemitsu *et al.*, 2005). Little genetic marker analysis has been done in a rat model during pregnancy induced cardiac hypertrophy.

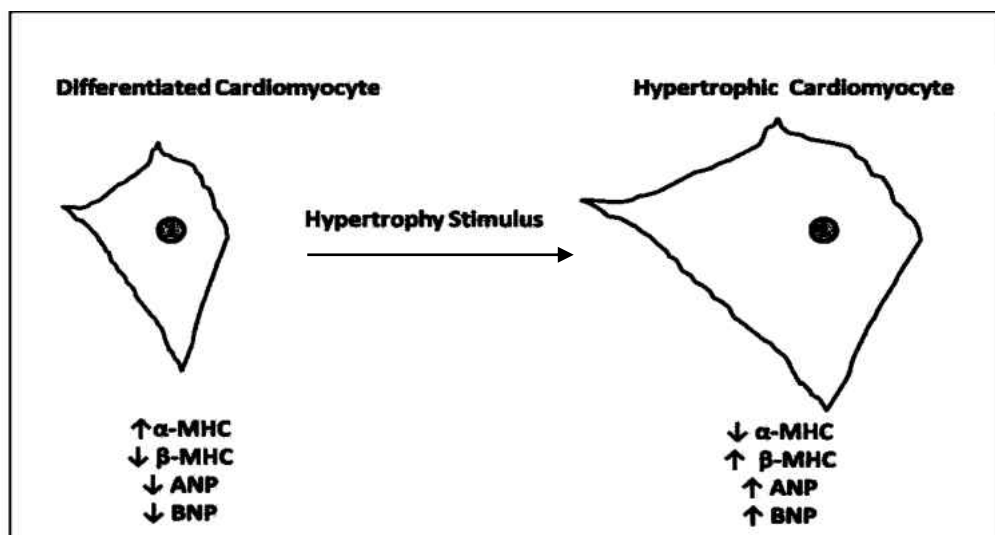


Figure 3. Schematic of the gene expression markers of hypertrophy. These markers are used as a standard to determine the degree of cardiac hypertrophy. An example of a differentiated cardiomyocyte would be one that is present in a healthy heart. Following a hypertrophy stimulus, such as high blood pressure, the cardiomyocytes in the heart enlarge to compensate for added stress. During this process, the genetic marker expression levels change through a series of complex molecular pathways. Information was compiled following a literature review.

α -MHC

Alpha myosin heavy chain (α -MHC) is a cardiac specific sarcomeric gene highly expressed in the atrial septum (Posch *et al.*, 2010). Myosin is the main component of the thick sarcomeric filament and uses ATP hydrolysis to produce force for contraction. Myosin motors act upon thin filaments composed of actin and troponin-tropomyosin regulatory complex. In resting muscle, when the calcium concentration is low, the regulatory proteins prevent myosin from contact with actin. During each heartbeat, calcium is released from the sarcoplasmic reticulum into the cytoplasm, where it binds to troponin and allows myosin to interact with actin filaments to produce a contraction. The muscle then relaxes as calcium is removed from the cytoplasm (Malik *et al.*, 2011). Alpha MHC is regulated by TBX5, which encodes a member of the family of T box transcription factors and expressed in the embryonic heart (Posch *et al.*, 2010). An increase in β -MHC expression and a decrease in α -MHC expression have been accepted cardiac hypertrophy markers for the past 40 years (Barry *et al.*, 2008). Each isoform has distinct enzymatic activity, which means that the relative ratios of activity greatly impact cardiac function (Barry *et al.*, 2008). For example, an increase in β -MHC decreases the myosin ATPase enzyme velocity, which then slows down the myosin contractile work (Barry *et al.*, 2008). This same mechanism occurs during an altered workload in the heart (Barry *et al.*, 2008). The cardiac remodeling process following hypertrophy is generally associated with the return of the MHC isoform levels back to normal (Barry *et al.*, 2008).

In pathological cases, such as those patients with dilated cardiomyopathy utilizing β -blocker therapy, the hypertrophy recovery is associated with an increase in α -MHC and a decrease in β -MHC (Barry *et al.*, 2008). Ching *et al.* did a protein-protein *in silico* study using a glutathione s-transferase (GST) tag pull-down assay and surface receptors to discover that a mutation in α -MHC causes an atrial septum defect (Ching *et al.*, 2005). A mutational scan of the coding regions for the α -MHC gene was completed recently in 470 congenital heart disease patients (Granados-Riveron *et al.*, 2010). This study identified that in congenital heart patients, the α -MHC gene contains a stop codon mutation, splice acceptor site mutation and 7 missense mutations (Granados-Riveron *et al.*, 2010).

Existing cardiac contractile drugs that affect myosin increase cardiac contractility indirectly. The use of these drugs is limited by adverse effects. Malik and colleagues created a small-molecule direct activator of cardiac myosin in order to avoid these effects (2011). They recently identified that the activator, omecamtiv mecarbil, binds to the myosin catalytic domain and operates by an allosteric mechanism to increase the transition rate of myosin into myosin bound with actin. In animal models, they identified that omecamtiv mecarbil increases cardiac function by increasing the duration of ejection without changing the rate of contraction (Malik *et al.*, 2011). This finding is applicable to systolic heart failure patients as a possible therapeutic option (Malik *et al.*, 2011).

It is still difficult to study the MHC isoforms using the rat, human and mouse models. A main complication in studying the MHC gene is in humans, 90% of the total MHC is of the beta isoform (Barry *et al.*, 2008). On the other hand, in rodents, the primary MHC isoform is alpha, most likely due to their high heart rate (Barry *et al.*, 2008). It is important to study the MHC in all three species. Caution should be taken when utilizing α -MHC results and relating to human disease for these specific reasons.

Natriuretic peptides: ANP and BNP

Natriuretic peptides are internally derived antagonists that are important in modulation of molecular mechanisms involved in metabolic regulation and cardiovascular remodeling (Savoia *et al.*, 2010). The four main types of natriuretic peptides include: atrial natriuretic peptide (ANP), brain natriuretic peptide (BNP), c-type natriuretic peptide (CNP) and dendroaspis natriuretic peptide (DNP) (Akashi *et al.*, 2007). All of these peptides share a common 17 amino acid cyclic structure, although the tails of ANP and BNP both have a 5' carboxy termini and an 3' amino termini, while CNP lacks the carboxy tail (Akashi *et al.*, 2007). ANP and BNP are found at high levels during embryonic development and in early neonates but are absent in healthy adults (Barry *et al.*, 2008). Currently, not much information is known regarding DNP and the connection to cardiovascular disease.

ANP and BNP are synthesized in the myocardium as their precursor pro-ANP and pro-BNP (Engle *et al.*, 2010; Moertl *et al.*, 2009). These segments are then cleaved into their corresponding biologically inactive amino-terminal segments of the precursor molecules by a cardiac protease either amino-terminal pro-atrial natriuretic peptide (NT-proANP) or amino-terminal pro-B type natriuretic peptide (NT-proBNP), both products are around 108 amino acids long, as seen in Figure 4 (Akashi *et al.*, 2007; Moertl *et al.*, 2009). This molecular split event also results in the active peptides to be released, ANP and BNP, both around 32 amino acids long (Hildebrandt, 2009; Akashi *et al.*, 2007).

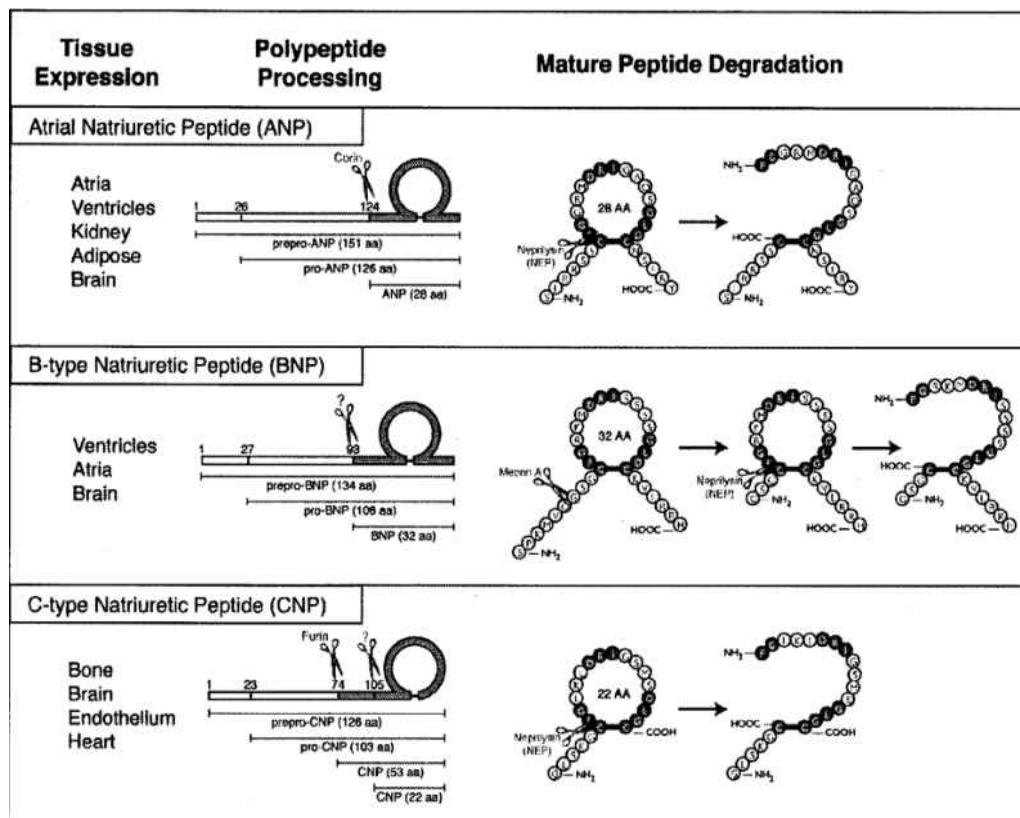


Figure 4. Processing of the natriuretic peptides. ANP, BNP and CNP all have short half-lives, making identification and analysis difficult. Their precursor proteins, pro-ANP, pro-BNP, and pro-CNP have much longer half-lives, making them ideal therapeutic targets.

Source: Potter, L.R., Yoder, A.R., Flora, D.R., Antos, L.K. and Dickey, D.M. (2009). Natriuretic peptides: their structures, receptors, physiologic functions and therapeutic applications. *cGMP: Generators, Effectors and Therapeutic Implications*, 341 Handbook of Experimental Pharmacology, Springer-Verlag Heidelberg.

The active natriuretic peptides then bind to one of three high affinity receptors, NPR-A, NPR-B, or NPR-C (Savoia *et al.*, 2010). NPR-A and NPR-B share similar structures, and are linked to the production of cyclic guanosine monophosphate (cGMP) (Savoia *et al.*, 2010). NPR-C has sequence similarities with the other two receptors, but lacks an intracellular catalytic domain of guanylate cyclase (Savoia *et al.*, 2010). Even with similar structures, all three receptors bind to different natriuretic peptides. NPR-A, primarily found in the kidneys and adrenal glands, binds to both ANP and BNP but has the highest affinity for ANP (Kasama *et al.*, 2008). NPR-B, found in brain and fibroblasts, binds to solely CNP (Savoia *et al.*, 2010). NPR-C, found in various tissues, kidneys and adipose tissue, binds to all three natriuretic peptides with the same affinity (Akashi *et al.*, 2007). NPR-C regulates the final ANP and BNP binding to NPR-A and as a final clearance receptor for all the peptides (Kasama *et al.*, 2008;Savoia *et al.*, 2010). ANP and BNP are also rapidly removed by this receptor (Savoia *et al.*, 2010).

The natriuretic peptides inhibit renin, vasopressin and aldosterone release (Savoia *et al.*, 2010). Renin mediates extracellular volume of plasma, blood, lymph, and interstitial fluid (Savoia *et al.*, 2010). Vasopressin is a peptide hormone that is an important contributor of blood pressure by regulating the vascular resistance including vasoconstriction (Savoia *et al.*, 2010). Lastly, aldosterone increases reabsorption of sodium ions and water, thus helping in increasing the blood volume and blood pressure (Savoia *et al.*, 2010). ANP and BNP production and secretion is regulated by complex interactions with both the neuro-hormonal and immune systems, especially in the ventricular myocardium (Akashi *et al.*, 2007). Stimulators that produce/secrete ANP or BNP include: glucocorticoids, sex steroid hormones, thyroid hormones, endothelin-1, angiotensin II, and cytokines, such as tumor necrosis factor- α , interleukin-1 and interleukin-6 (Akashi *et al.*, 2007). The natriuretic peptides can be inactivated through several different inactivation pathways: enzymatic degradation by neutral endopeptidase, or NEP, or through lysosomal degradation after uptake by a clearance receptor, such as NPR-C (Akashi *et al.*, 2007).

During heart failure, natriuretic peptide levels in plasma not only are used as a diagnostic, but can also be used to determine the severity of the disease and its prognosis

in both clinical and laboratory studies (Moertl *et al.*, 2009). Elevation of BNP, for example, is a key feature of cardiovascular damage in obese patients (Savoia *et al.*, 2010). Obesity decreases the bioactive levels of natriuretic peptides via the increased expression of the clearance receptor NPR-C in adipose tissue (Savoia *et al.*, 2010). This may potentiate adipogenesis and lipid accumulation (Savoia *et al.*, 2010). Animal and human adipose tissues express both NPR-A and NPR-C, but in obese patients, the ratio between the two is reduced (Savoia *et al.*, 2010). Deletion of ANP in mice causes hypertension and hypertrophy under resting conditions (Barry *et al.*, 2008). Deregulation of natriuretic peptides is involved in pathogenesis of left ventricular hypertrophy in patients, as studies have shown that as levels of ANP are inversely related to left ventricular mass (Savoia *et al.*, 2010). Recently, Magnusson *et al.* conducted a direct comparison of NT-BNP, BNP and NT-ANP levels and showed evidence that all three could be potential prognostic indicators of hypertrophy (2009).

Although the natriuretic peptides, especially ANP and BNP, have been established as potential prognostic tools, issues arise that might suggest utilizing their precursors, pro-ANP and pro-BNP instead. For example, the BNP peptide has a half-life of 12 to 22 minutes, while its precursor, NT-proBNP, has a half-life of 60 to 90 minutes (Moertl *et al.*, 2009). NT-proBNP is often subject to degradation and polymerization, so the amino end is usually not useful for assays (Moertl *et al.*, 2009). The ANP peptide's half-life is a mere 2 to 5 minutes, too short for any clinical application (Moertl *et al.*, 2009). NT-proANPs half-life is longer than the hormone itself, but still too short for diagnostic purposes (Moertl *et al.*, 2009). BNP and pro-BNP are useful in diagnostic settings, especially with those patients with congestive heart failure (Tsai *et al.*, 2010). Out of the two peptides, BNP is more commonly used, but with caution; often common prescription medications alter peptide levels, especially those that are the angiotensin-converting enzyme inhibitors and angiotensin II blockers (Hildebrandt, 2009 & Wang *et al.*, 2010). The Food and Drug Administration (FDA) approved a cutoff value for BNP in congestive heart failure patients to be 100 pg/mL (Tsai *et al.*, 2010).

miRNAs

MicroRNA's (miRNA or miR) are short, endogenous, non-coding, single stranded segments of RNA that regulate gene expression through hybridization to messenger RNA (mRNA). The terminal consequence of miRs binding to mRNA is mRNA degradation or translational inhibition of targeted transcripts (Zhang *et al.*, 2011). MiRNAs can be excised from within introns of non-protein or protein coding transcriptional units or even within genomic repeats (Zhao & Srivastava, 2007). Not only can an individual miRNA target dozen mRNAs, but also a single mRNA can be complementary to multiple miRNA (van Rooij *et al.*, 2008). A recent estimate approximates the total possible miRNAs in the human genome to consist of 3% of the human genome; of which then regulates approximately 30% of the entire human genome (Boštjančič, 2010, Shen *et al.*, 2010). Since the first discovery of miRNA let-7 in *Caenorhabditis elegans* 10 years ago, over 900 microRNAs have been identified, cloned, and sequenced (van Rooij *et al.*, 2007). MiRNA have become of such interest since the discovery of let-7 because miRNA have been identified to be important regulators in processes such as cell differentiation, growth, proliferation and apoptosis (Lagos-Qunitana *et al.*, 2003, Zhang, 2008). Many miRNAs, especially those expressed in tissue, regulate developmental and physiological functions, such as the following: stem cell differentiation, neurogenesis, hematopoiesis, immune functions, and metabolism (Boštjančič, 2010). The miRNA identified could also be responsible for diseases such as cancer, autoimmune, inflammatory, and cardiovascular disorders (Boštjančič, 2010).

MiRNA Processing

MiRNAs are initially transcribed by RNA polymerase II or III in the nucleus to form large pri-miRNA transcripts, as shown in Figure 5 (Zhang, 2008). These miRNA precursors are usually several kilobases long and then capped and adenylated (Callis, Chen & Wang, 2007). The pri-miRNAs are processed and cut in the nucleus by RNase III enzyme Drosha (also identified as RNASEN) and the double stranded RNA (dsRNA) binding protein Pasha (also identified as DGCR8, or DiGeorge Critical Region 8); resulting in approximately 70-90 nucleotide pre-miRNAs which fold into a stem-loop hairpin structure (Zorio *et al.*, 2009; Cai *et al.*, 2010). From here, the pre-miRNAs can be transported out of the nucleus and into the cytoplasm by RanGTP and exportin 5 (Yang

et al., 2009; Wang, Zhou, Liao & Zhang, 2009). Subsequently, another enzyme, RNase III Dicer, processes the pre-miRNA to generate a 18-24 nucleotide duplex.

The final step occurs when the duplex is loaded into the miRNA associated miRISC (RNA-induced silencing complex) (Zhang, 2008). One strand of the miRNA is retained in the complex and becomes a mature miRNA, the opposite strand is eliminated (Zhang, 2008).

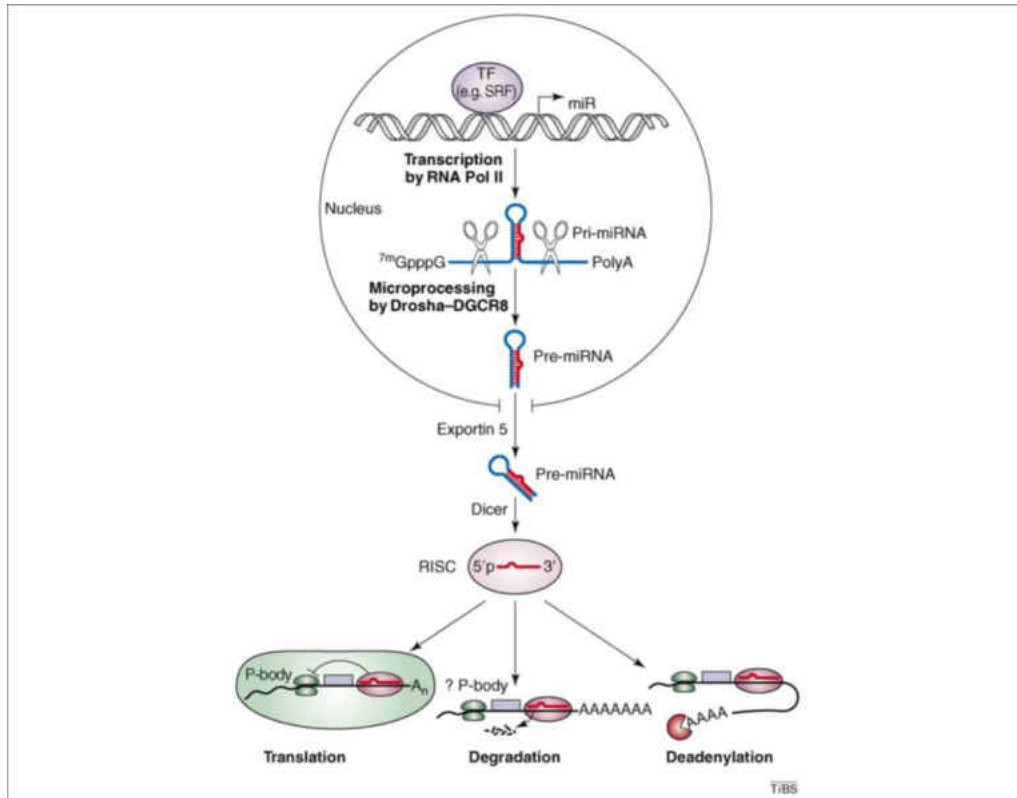


Figure 5. Schematic of miRNA activation. This process initially takes place in the nucleus prior to the pre-miRNA product being exported. After binding to RISC, or the RNA Induced Silencing Complex, the mature miRNA can then repress translation, bind to the complementary mRNA to target for degradation, or be further modified through deadenylation.

Source: Zhao, Y. and Srivastava, D. (2007). A developmental view of microRNA function. *TIBS*, 32, 189-197.

The mature miRNA then anneals to a 3' un-translated region of the target mRNA, where it promotes translational repression or mRNA degradation (van Rooij *et al.*, 2008). The pre-miRNA can also be further modified by adenosine deamination, which can

further control targeting specificity as well as modulate the stability and processing of the miRNA precursor transcript (Catalucci et al., 2008). Recent studies have highlighted that tumor suppressor p53 modulates miRNA processing through interactions with Drosha (Suzuki & Miyazono, 2010).

MicroRNAs that base pair perfectly with target mRNA sequences result in mRNA degradation, whereas those with imperfect sequence complementarities with mRNA sequences result in either direct or indirect degradation (Yang *et al.*, 2009, Zorio *et al.*, 2009). Single miRNA targets may function according to a ‘combinational circuitry model’, whereby a single mRNA targets multiple mRNAs and several co-expressed miRNAs may target a single mRNA (Carè *et al.*, 2007).

The importance of the RNase enzyme dicer has been extensively studied utilizing transgenic mouse models. Callis & Wang in 2008 studied the outcome after deletion of Dicer in both mouse and zebrafish. When the dicer function was disrupted in the mouse, the mouse stopped development during gastrulation before the body plan was completed (Callis & Wang, 2008). In zebrafish the fish experienced abnormal morphogenesis and heart development abnormalities (Callis & Wang, 2008). These results demonstrated that miRNA are important in the developmental stages. A similar result was seen in dicer knockout pups, as they died at post-natal day 4 (Prasad *et al.*, 2009). Dicer is the only enzyme involved in the maturation of miRNAs from their precursor, so when down-regulated, the miRNA expression level is also decreased (Chen *et al.*, 2007; Prasad *et al.*, 2009). When dicer was deleted using cre-recombinase, which is controlled predominantly by the α -MHC promoter, the hearts exhibited different cardiac contractile protein expression and sarcomeric disarray (Callis & Wang, 2008). This disarray led to a decrease in cardiac function, which progressed quickly into heart failure (Callis & Wang, 2008). A study conducted by Saxena & Tabin in 2010 demonstrated that dicer is necessary for cardiac outflow and chamber septation.

The miRNA nomenclature system not only designates information regarding the order of discovery, but gives clues regarding the precursors involved during the modification steps. For example, miRNAs that are encoded by more than one loci are

differentiated by numerical suffixes, such as miR-1-1 and miR-1-2. MiRNAs that only differ in the number of bases and are also derived from the same loci are denoted by alphabetical suffixes, such as miR133a and miR133b. Lastly, miRNA that are derived from the same precursor, but with different tissue-specific post-transcriptional maturation are denoted by adding which arm of the hairpin loop they were derived from, such as miR-126-5p and miR-126-3p, which are derived from the 3' and 5' arms, respectively (Zorio *et al.*, 2009).

Identification of miRNA Targets

In order to completely understand the molecular functions of miRNAs, it is important to identify their mRNA targets (Callis & Wang, 2008). The identification of miRNA targets is a complicated process because they act as a concerted effort in a complex molecular network (Shen *et al.*, 2010). The current understanding of these targets is based on computational target predictions and empirical information regarding the developmental expression patterns and evolutionary conservation (Shen *et al.*, 2010). These computational programs work to match the animal miRNAs to the complementary target sites through complementary sequence searches (Callis & Wang, 2008).

The portion of the miRNA that must complement to the mRNA sequence are nucleotides 2 through 8 on the 5' end, also called the seed sequence (van Rooij *et al.*, 2008). Generally, matching the seed sequence to the complementary mRNA sequence is accurate; however, other nucleotides and mRNA secondary structures in regions surrounding the target can also influence the association of the miRNA and mRNA (van Rooij *et al.*, 2008). After a systematic analysis by Friedman *et al.* in 2010, they determined that the seed region is the key determinant of miRNA specificity.

Bioinformatics has been of great use to identify miRNA targets through sequence alignments. MiR-base (<http://www.miRbase.org>) has a variety of different resources, such as the microcosm, which provides target prediction services. MirBase also links miRNAs to targets predicted by microcosm, Target Scan, and Pictar. Target Scan (<http://www.targetscan.org>) is of use to determine microRNA targets in mammals,

including the mouse, worm and fly. This program predicts biological targets of miRNAs by searching the seed region of each miRNA.

Through utilizing <http://www.targetscan.org>, we identified miRNA that bind to the myosin heavy chain (human MYH6, gene ID: 4624 in PubMed). These miRNA include: miR1827, miR1294, miR31, miR-182, miR-552, miR-556-3p and miR-1279.

miRNAs and Cardiovascular Disease

MiRNA are important in cardiovascular development, vascular angiogenesis, hypertrophy and cardiovascular disease (Shen *et al.*, 2010). MiRNAs such as miR-21, miR-195, miR-133 and miR-208 play a role in the process of cardiac remodeling by regulating changes in gene expression that accompany pathological disorders (Sucharov *et al.*, 2008). More information regarding these miRNA can be found in Table 2.

Table 2. miRNA expression profiles for miR-1, miR-133a, miR-195 and miR-21 assembled through a literature review. Although these miRNA have been identified to play a role during pathological hypertrophy, little is still known regarding their targets and downstream effects.

miRNA	Pathological Hypertrophy Response	Function	Targets
1	Downregulated	<ul style="list-style-type: none"> • Cardiomyocyte apoptosis • Late stage differentiation of growth cartilage cells • Cardiac development and differentiation • Cell growth • Calcium dependent signaling 	<ul style="list-style-type: none"> • Hand-2 • Ras-GAP • Cdk9 • Rheb • Fibronectin • TWF1 • HCN2 • HCN4
133a	Downregulated	<ul style="list-style-type: none"> • Apoptosis 	<ul style="list-style-type: none"> • HCN2 • SRF • RhoA • Cdc42 • Nelf-A/WHSC2
195	Upregulated	<ul style="list-style-type: none"> • Angiogenesis under hypoxia 	None Identified
21	Upregulated	<ul style="list-style-type: none"> • Unclear • Stimulate cell growth? • Activate apoptosis? • Inhibit cell cycle proliferation? • Modify signaling pathways? 	<ul style="list-style-type: none"> • SPRY1 • TPMI

MiRNAs have also been identified that play a role in physiological cardiac hypertrophy in mice (Shen *et al.*, 2010). MiRNAs 1, 133 and 150 have been shown to be anti-hypertrophic, while miRNAs-195, 21, 18b, 23a, 23b, 24, 181b and 214 are pro-hypertrophic (Shen *et al.*, 2010). A miRNA array showed that more than 80% of the 350 miRNAs examined in a mouse model were either up-regulated or down-regulated in the failing heart when compared to the control mice (Latronico *et al.*, 2008). Failing human hearts have showed increased expression of miR-24, miR-125b, miR-195, miR-199a and miR-214 (van Rooij *et al.*, 2006, van Rooij *et al.*, 2008).

miRNA Expression During Cardiac Remodeling

MiRNA in the mouse model identified to be responsible for post-hypertrophy cardiac remodeling include: 347, 483, 326, 212, 130b, 29a, and 23a (Wang *et al.*, 2009). Two particular miRNA that are of interest are miR-23a and miR-29. MiR-23a was identified to be down-regulated during hypertrophy and up-regulated during the remodeling process (Wang *et al.*, 2009). MiR-29 was identified to be down-regulated by greater than two fold during hypertrophy but gradually up-regulated up to 1.5 fold during cardiac remodeling (Wang *et al.*, 2009). To date, there have not been any experiments looking into the miRNA expression during pregnancy induced cardiac hypertrophy as well as the remodeling process.

miR-21

MiRNA-21 is involved in tumor-related cell growth and apoptosis, mediation of signaling pathways in neonatal cardiomyocytes, and much more (Shen *et al.*, 2010). The exact function of this miRNA still remains unclear (Shen *et al.*, 2010). MiR-21 has a pro-proliferative and anti-apoptotic effect on muscle cells (Zhang, 2008). It is still unknown exactly what role miR-21 has on apoptosis, as it is still very contradictory (Zhang, 2008). Studies have shown that miRNA 21 stimulates cell growth, while others find that miRNA 21 activates apoptosis and inhibits cellular proliferation (Callis & Wang, 2008). It has been accepted, however, that miR-21 is up-regulated during pathological cardiac hypertrophy (Zhang, 2008).

In order to determine the mRNA target and molecular function of miR-21, transgenic mice, and cell culture lines have been used. After inhibition of miR-21 and miR-18b in neonatal rat cardiomyocytes, lab results identified an induction of hypertrophy and an increase in cardiomyocyte size (Tatsuguchi *et al.*, 2007). Utilizing *in situ* hybridization, miR-21 was detected in very small amounts in normal myocardium, but higher levels in failing myocardium (Thum *et al.*, 2008). In another transgenic model, knockdown of miR-21 repressed cardiomyocyte growth and fetal gene expression in response to hypertrophic agonists (Shen *et al.*, 2010). Another study utilized knockout mice to determine that in the absence of miR-21, stress dependent cardiac remodeling occurs (Patrick *et al.*, 2010). Although the mRNA target for miR-21 has yet to be identified, recent knockout models suggest that miR-21 targets SPRY1, a potential inhibitor of the RAS/MEK/ERK pathway (Thum *et al.*, 2008). Other direct targets of miR-21 in fibroblasts are phosphatase and tension homologue (PTEN), a lipid and protein phosphatase that negatively regulates the P13K signaling pathway (Haghikia & Hilfiker-Kleiner, 2009). PTEN also affects other cellular features such as survival, growth, metabolism, protein synthesis, and secretory activity (Haghikia & Hilfiker-Kleiner, 2009).

miR-195

During pathological hypertrophy, miR-195 is up-regulated in both human and mouse. Expression is sufficient to induce hypertrophic growth in cultured rat cardiomyocytes (Callis & Wang, 2008). MiR-195 can also rescue cell division in stem cells by suppression of WEE1 and p21 (Shen *et al.*, 2010). A reason this occurred could be because miR-195 attenuates the cell cycle by down-regulating cyclin D1, cdk6, and E2F3 (Shen *et al.*, 2010).

MiR-195 is one of the few miRNA in which the functional target has yet to be identified. Over-expression of miR-195 increases the left ventricular wall size, which then up-regulates the expression of ANP, BNP and β -MHC, which then consequently reduces cardiac output (Shen *et al.*, 2010). Over-expression of miR-195, results in dilated cardiomyopathy and heart failure in mice as early as 2 weeks old (van Rooij *et al.*,

2008). In another study, over-expression of miR-195 was enough to induce cardiac dysfunction and heart failure in transgenic mice (Shen *et al.*, 2010).

miR-1

MiRNA-1 is considered pro-apoptosis through repressing heat shock proteins HSP60 and HSP70 without altering transcript levels (Shen *et al.*, 2010). Excess of miR-1 in developing cardiac tissue leads to a decreased pool of proliferating cardiomyocytes; thus supporting the hypothesis that miR-1 genes control the balance between differentiation and proliferation during cardiogenesis (Mishra *et al.*, 2009). Other literature has stated that miR-1 inhibits cardiomyocyte proliferation (van Rooij *et al.*, 2008).

MiRNA-1 is a muscle specific miRNA and expression is often seen as early as embryonic day 8.5 (Sayed *et al.*, 2007). Overexpression of miR-1 in developing mice heart caused defective ventricular myocyte proliferation (Callis *et al.*, 2009). Typically when fetal gene marker β -MHC is over-expressed, miR-1 inhibits myocyte proliferation and cardiac development, suggesting a relationship between the fetal gene markers and miRNA (Sayed *et al.*, 2007). Mice deficient in miR-1 display abnormalities in the cellular hyperplasia (Bauersachs & Thum, 2007). MiRNA-1 has also been noted to regulate twinfilin-1, or TWF-1, a cytoskeleton regulatory protein (Li *et al.*, 2010).

In mice, miR-1 expression decreases in the early stages of hypertrophy (Sayed *et al.*, 2007). In fact, just one day after TAC surgery, miR-1 was down-regulated and continued to be down-regulated through day 7 (Shen *et al.*, 2010). The reason for this is that miR-1 directly targets Ras GTPase activating protein (Ras GTP), cyclic-dependant kinase (cdk9), Ras homolog enriched in brain (Rheb) and fibronectin, all of which contribute to the onset of cardiac hypertrophy (Shen *et al.*, 2010). Another verified target for miR-1 is the cardiac transcription factor Hand-2, which is connected to cardiac growth during embryogenesis (Callis & Wang, 2008). In studies confirming this, miR-1 overexpression reduced the levels of Hand-2, and Hand-2 levels were increased in miR-1-2 null animals (Callis & Wang, 2008).

MiR-1 activity is transcriptionally regulated by myogenic differentiating factors, such as myogenic differentiation 1 (MyoD), myocyte enhancing factor 2 (Mef2), and serum response factor (SRF) (Zorio *et al.*, 2009). This regulation is tissue specific; as miR-1 is controlled by SRF in the heart but Mef2 and MyoD in skeletal muscles (Zorio *et al.*, 2009). SRF is a transcription factor that recruits co-activators and myocardin to muscle specific genes that control differentiation (Callis *et al.*, 2009; Zhang *et al.*, 2011). MiR-1 also represses the expression of histone deacetylase (HDA4), which acts as a signal dependent repressor of Mef2 (van Rooij *et al.*, 2008).

miR-133a

MiR-133a is down-regulated in human heart disease and deregulated during both physiological and pathological hypertrophy (van Rooij *et al.*, 2006; van Rooij & Olson, 2007; van Rooij *et al.*, 2008). Results are contradictory on miR-133a's response to apoptosis. For example, one report states that it promotes myoblast proliferation and apoptosis, while others report that it is anti-apoptotic (Boštjančič, 2010; Shen *et al.*, 2010).

Mir-133a suppresses SRF, an important regulator of muscle differentiation (van Rooij *et al.*, 2008). SRF also interacts to control the stress-induced fetal gene reactivation during hypertrophy (Ahmad *et al.*, 2005). Mir-133a also represses translation of polypyrimidine tract binding protein PTB, which promotes the differential splicing of a variety of transcripts (van Rooij *et al.*, 2008). The target genes for miR-133a are Rhoa, a GDP-GTP exchange protein regulating cardiac hypertrophy, Cdc42, a signal transduction kinase, and WhSc2, a nuclear factor involved in cardiogenesis (Bauersachs & Thum, 2007). In hypertrophied mice hearts, the expression of mir-133a was inversely related to the expression of all of those proteins (Bauersachs & Thum, 2007). This information was confirmed again through the use of a luciferase assay, in which the luciferase reporter gene was linked to the wild type 3' UTR of Rhoa, Cdc42, and Whsc2 (Bauersachs & Thum, 2007). This resulted in a significant decrease in luciferase activity, thus confirming their role as targets (Bauersachs & Thum, 2007).

miR-1 and miR-133a

MiR-1 and miR-133a are produced from the same polycistronic transcripts and are encoded by two separate genes in the genomes of the mouse and human (Callis & Wang, 2008). These miRNA's are highly conserved and are also expressed in the muscle of flies, mice, and humans (Callis & Wang, 2008). Both miRNAs have muscle specific expression patterns that promote myoblast differentiation (Boštjančič, 2010). MiRNA 1 and 133a have been shown to be closely involved in regulating cardiomyocyte apoptosis (Shen *et al.*, 2010). Both miR-1 and miR-133a promote differentiation and proliferation of cardiac and skeletal muscle cells (Shen *et al.*, 2010). These miRNA have also been assessed in hypertrophy models and human heart disease (Shen *et al.*, 2010). This model suggests that miR-1 and miR-133a expression levels are significantly reduced in cardiac hypertrophy, indicating a reverse correlation between miR-133a and miR-1 expression and myocardial hypertrophy (Shen *et al.*, 2010).

MiR-1 and MiR-133a work in a system is also referred to as MADS (MCM1 agamous deficiens serum response factor box) (van Rooij *et al.*, 2008). The transcription factors for the MADS box are SRF and Mef2, both of which regulate muscle cell proliferation and differentiation through interactions with other transcription regulators (van Rooij *et al.*, 2008). SRF and Mef2 control the expression levels of miR-1-1/133a-2 and miR-1-2/133a-1 (van Rooij *et al.*, 2008). SRF and Mef2 cooperate with MyoD to activate transcription of factors (van Rooij *et al.*, 2008).

MiR-1 and miR-133a regulate the cardiac conduction system components and induce arrhythmia (Shen *et al.*, 2010). In fact, miR-1 overexpression slowed the conductance and depolarized the cytoplasmic membrane by post-transcriptionally repressing KCNJ2, which encodes the potassium channel subunit, and GJA1, which encodes connexin 43, thus leading to severe cardiac arrhythmias (Bauersachs & Thum, 2007). Using this information, scientists have been able to identify potential target sites for both miR-1 and miR-133a. HCN2, or hyperpolarization activated cyclic nucleotide gated potassium channel 2, and HCN4 are both pacemaker channel control genes and

have been identified as potential repression targets for miR-1 (Luo *et al.*, 2008). HCN2 is a potential repression target for miR-133a (Luo *et al.*, 2008).

Potential Therapeutic Applications

MiRNAs have sparked interest because of their potential in studying gene function, validating diagnostic biomarkers, confirming candidate drug targets, and perhaps even treating certain diseases (Zorio *et al.*, 2009). MiRNA targets are pursued for treatment options for Alzheimer's Disease, Parkinson's Disease, cancer, diabetes, heart failure, and many more. In fact, miRNA are now being called "onco-miRs." Another possibility for the use of miRNA is designing new protocols for manipulating miRNAs. For example, prevention of lower miR-195 expression during hypertrophy could prevent the heart from going into heart failure (van Rooij *et al.*, 2008). Knockout of specific miRNA, such as miR-1 and miR-133 could help facilitate the remodeling process (van Rooij *et al.*, 2008).

Species Specific Differences between the Rat, Mouse, and Human

Rattus norvegicus was the first mammalian species to be used for laboratory work (Jacob & Kwitek, 2002). The mouse was more commonly used in the laboratory for mammalian geneticists because scientists preferred the small size and range of coat colors (Jacob & Kwitek, 2002). Most rat models have phenotypic characteristics relevant to a human condition, such as those for hypertension; however, it is nearly impossible to recapitulate clinical outcomes of human disease due to sex-specific differences (Jacob & Kwitek, 2002).

Other issues arise with rat or mouse models in that these species often do not all the clinical symptoms of human disease (Jacob & Kwitek, 2002). Studies done in these species, especially in a single inbred rodent strain, often fail to sample a sufficient amount of genetic diversity to account for the complex phenotype (Jacob & Kwitek, 2002). For example, several years ago, a rat gene that was mapped near the angiotensin-converting enzyme (ACE) gene was thought to be responsible for hypertension (Jacob &

Kwitek, 2002). Further studies demonstrated that ACE was not linked to hypertension in humans (Jacob & Kwitek, 2002).

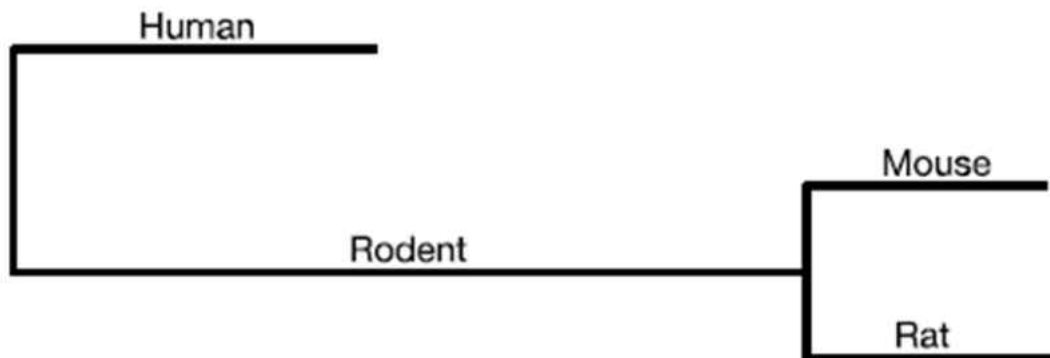


Figure 6. Phylogenetic relationship between three species. Even after the development of new technology and bioinformatics techniques using sequence alignments, a phylogenetic relationship has not yet been clearly defined between the mouse and rat. Learning more about the differences between the species could open doors regarding finding the ideal model organism to study pathological diseases.

Source Rat Genome Sequencing Project Consortium. (2004). Genome sequence of the brown Norway rat yields Insights into mammalian evolution. *Nature*, 428, 493-520.

The Rat Genome Sequencing Project Consortium (RGSPC) in 2004 examined the rat, mouse, and human genomes to compare and evaluate evolutionary trends. The phylogenetic tree they agreed is in Figure 6. The RGSPC found that some genes in the rat, but not mouse, arose from the expansion of common gene families. These include those that produce pheromones, immunity, chemosensation, detoxification and proteolysis. They also identified that almost all human genes have known to be associated with disease have orthologous in the rat genome.

The RGSPC looked at the X chromosome for divergence events between the three animals. The X chromosome consists of 16 human/mouse/rat orthologous genes that are at least 300 kb in size. The committee counted a total of 15 inversions in the genome in the descent from primate to rodent to ancestor. They also identified 278 orthologous genes between the human and rat and 280 between the human and mouse, thus supporting the hypothesis that the species are closely related. The RGSPC identified 454 non-coding RNA (ncRNA), of which 113 were miRNA.

Looking through evolutionary time, the RGSPC found that 90% of rat genes possess strict orthologous genes in both the mouse and human genomes. In-paralogs have arisen from recent duplication events occur only in the rat, and not mouse and human. While using a rat model is sufficient for studying molecular signaling pathways, it is important to recognize that even if the species are evolutionary related, species-specific differences will still occur (Jacob & Kwitek, 2002).

Chapter 2

Materials and Methods

This study was conducted between February 2010 to April 2011 at Eastern Kentucky University located in Richmond, Kentucky. Eastern Kentucky University's Institutional Animal Care and Use Committee (IACUC) approved this project (Holden 04-2010). The approval letter can be found in Appendix 1.

Specific Aim 1: Morphological Characterization of Pregnancy Induced Cardiac Hypertrophy and Post-Partum Remodeling.

Rodent Use

Sprague Dawley rats were ordered at 8 weeks old through Charles River (Wilmington, MA). Rats were allowed to acclimate to our animal facility for the standard 1 week. Rats were subjected to timed matings at approximately 9 weeks old. Male rats were placed into female rat cages at approximately 5pm and removed at 10am the following day. Approximately two-weeks after mating, females were split into three groups: not pregnant (NP, n=18), 19 days pregnant (P, n=8), and 24 hours post-pregnant (PP, n=9). Pregnancy can be determined visually at approximately 14 days gestation. At the appropriate time points, animals were euthanized in a euthanasia chamber utilizing approximately 5 mL isoflurane (Allivet, St. Hialeah, FL). Immediately following euthanasia, heart weight, body weight, and tibia length (mm) were all noted. The apex of the heart, primarily left ventricle, was stored in a 15 mL conical tube with 5 mL RNA later (Invitrogen, Carlsbad, CA) for RNA extraction. The base (top most part) of the heart was fixed in 4% paraformaldehyde (Fischer Scientific, Pittsburg, PA) for 48 hours. Following fixation of tissue in paraformaldehyde, samples were stored indefinitely in 75% ethanol at 4°C.

Histology

Processing, sectioning, and Hematoxylin and Eosin staining (H&E) of the formalin- fixed base top of the heart were completed by the University of Kentucky Histology and Imaging Facility.

The processing of the histological samples were done by the following protocol, all steps were completed *in vacuo*: the samples were first processed in 75% ethyl alcohol for 30 minutes; then 85% ethyl alcohol for 30 minutes; 95% ethyl alcohol for 30 minutes, repeated twice; 100% ethyl alcohol for 30 minutes, repeated twice; lastly, xylene for 30 minutes, repeated three times. The processed samples were then embedded in Paraplast Plus for sectioning at 60°C three times for 30 minutes. Samples were cut into sections of 5 µm thickness.

H&E staining was completed on 1 slide with 3 to 5 sections. The following protocol was utilized, courtesy of Cynthia Long at the University of Kentucky Histology and Imaging Center: xylene for 5 minutes, xylene for 2 minutes, absolute ethyl alcohol for 2 minutes, absolute alcohol for 2 minutes, 95% alcohol for 2 minutes, 85% alcohol for 2 minutes, 70% alcohol for 2 minutes, stationary tap water for 2 minute, Hematoxylin for 2 minutes, running tap water for 2 minutes, scott's tap water (alternate blueing solution) for 30 seconds, running tap water for 2 minutes, 85% alcohol for 1 minute, 85% alcohol again for 1 minute, Eosin for 30 seconds, 95% alcohol for 30 seconds, 95% alcohol for 1 minute, 95% alcohol for 1 minute, absolute alcohol for 1 minute, absolute alcohol for 1 minute, xylene for 2 minutes, xylene again for 2 minutes, and xylene for 10 to 15 minutes.

Cardiomyocyte cell areas for all NP, P, and PP H&E stained samples were examined at 40x magnification utilizing Nikon NIS Elements 3.2 software (Nikon, Melville, NY).

Statistical Analysis

Statistical significance was analyzed using one way Analysis of Variance (ANOVA) for all data, including: heart weight to body weight, heart weight to tibia length, and cardiomyocyte area. A P-value of < 0.05 was considered to be significant.

Specific Aim 2: Expression of Known Hypertrophy Genes in Pregnancy and Post-Partum.

RNA Extraction

RNA was extracted from the apex of the rat hearts utilizing Trizol LS (Invitrogen, Carlsbad, CA), the Fast Prep 24 instrument (MP Biomedicals, Solon, OH), and the Fast Prep 24 Green Lysing Kit (MP Biomedicals, Solon, OH). The protocol was adapted from Dr. Rebekah Waikel's at Eastern Kentucky University and can be found in Appendix 2.

The apex of each heart was placed into a Fast Prep 24 Green Kit 2 mL tubes (MP Biomedicals, Solon, OH) containing 1.4 mm ceramic spheres; 1 mL of Trizol LS was then added to each tube. The tubes were then placed into the Fast Prep 24 machine and the machine was set at the following: speed 6, time 30 seconds, repeat 4 times. The samples were then centrifuged at low speed, 5000 rpm for 1 minute and the supernatant was transferred to a fresh tube. The tubes were then incubated, with rocking, for 5 minutes at room temperature at 100rpm. The samples were then centrifuged at 12,000xg for 10 minutes at 4°C, and the supernatant was transferred to a fresh tube. To the supernatant, 0.2 mL of Molecular Biology grade chloroform (MP Biomedicals, Solon, OH) was added; samples were vigorously shaken by hand for 15 seconds, and incubated at room temperature for 3 minutes with rocking at 100rpm. Centrifugation was repeated, at 12,000xg for 15 minutes at 4°C. The colorless upper aqueous phase was mixed with 0.5 mL Molecular Biology grade isopropanol (Fischer Scientific, Pittsburg, PA) in a new 1.5 mL tube. The samples were then incubated for at least 30 minutes on ice.

After the incubation period, the samples were centrifuged at 12,000xg for 10 minutes at 4°C. The supernatant was removed and the RNA pellet was washed with 1 mL Molecular Biology grade 75% ethanol (Fischer Scientific, Pittsburg, PA). The tubes were centrifuged at 7,500xg for 10 minutes at 4°C. The supernatant was then removed. The RNA pellets air-dried for 5 minutes. The pellet was then re-suspended with 100 µl Nuclease free water (Fisher Scientific, Pittsburg, PA) if a RNA pellet was visible, or 50 µl Nuclease free water if a RNA pellet was not present.

RNA quality was then determined through a UV Spectroscopy utilizing a 1:100 dilution in the Eppendorf Biophotometer Plus (Eppendorf, Hamburg, Germany) as well as gel electrophoresis. The RNA concentration, 260/280 and 230 A values were all

recorded to assess purity. A 260/280 value of approximately 2.0 was used to denote pure RNA. A 260/230 value of 2.0 to 2.2 designated pure RNA. The RNA was run on a 1% agarose gel at a concentration of 1 µg/µl. After assessing quality, RNA was stored at -70°C.

RNA conversion to cDNA (RT reaction)

Total RNA was converted to cDNA through reverse transcription utilizing the High Capacity cDNA Reverse Transcription Kit (Applied Biosystems, Carlsbad, CA). A master mix was made of the following components per reaction, as provided in the kit: 2.0 µl RT Buffer, 0.8 µl 25x dNTP Mix (100 mM), 2.0 µl 10x RT Random Primers, 1.0 µl Multiscribe Reverse Transcriptase and 1.0 µl RNase Inhibitor (if available). To each PCR tube, 5.8 µl of Master Mix was added. RNA concentration of 1 µg/µl was used to complete the reverse transcription (RT) reaction. The volume of the reaction was then brought to a total of 20 µl with nuclease free water.

The samples were placed in a MyCycler™ Personal Thermal Cycler (Biorad, Hercules, CA). As specified in the High Capacity cDNA Reverse Transcription Kit protocol, the thermal cycler was set for the following program: 25°C for 10 minutes, 37°C for 120 minutes, 85°C for 5 seconds, and 4°C to hold. All cDNA samples were placed in a -20°C freezer for storage.

Real Time PCR

A Real Time PCR reaction was completed following the cDNA reaction for the following genes: Glyceraldehyde 3-phosphate dehydrogenase (GAPDH), Natriuretic peptide precursor A (NPPA or ANP), Natriuretic peptide precursor B (NPPB or BNP), G-

Table 3. Primer sets utilized for Gene Expression Real Time PCR. All primer sets were purchased through Applied Biosystems (Carlsbad, CA). All primer sets were produced by Taqman®.

Name	Gene Name	Assay ID	Ref Seq	Amplicon Length (nt)
GAPDH	Glyceraldehyde 3-phosphate-dehydrogenase	Rn99999916_s1	NM_017008.3	87
GPER	G-protein-coupled estrogen receptor 1	Rn00592091_s1	NM_133573.1	102
NPPA	Natriuretic peptide precursor A	Rn00561661_m1	NM_012612.2	58
NPPB	Natriuretic peptide precursor B	Rn00676450_g1	NM_031545.1	93
MHC-α	Myosin Heavy Chain 6, cardiac muscle, alpha	Rn00691721_g1	NM_017239.2	71

protein coupled receptor 1 (GPER) and Myosin heavy chain 6, cardiac muscle, alpha (α -MHC). All primer sets were purchased from Applied Biosystems (Carlsbad, CA), primer set information can be found in Table 3.

All samples were done in triplicate. In a 1.5 mL tube, a Master Mix was made by combining the following, also accounting for the number of samples and triplicates: 1.0 μ L 20x Taqman® Gene Expression Assays (primer details shown above), 10.0 μ L 2x Taqman® Gene Expression Master Mix, and 8 μ L nuclease free water.

A MicroAmp® Fast Optical 48 well plate (Applied Biosystems, Carlsbad, CA) was used. To each well, 19 μ L Master Mix was added. Precisely 1 μ L cDNA product was added into the 19 μ L Master Mix and mixed well by pipetting up and down. The plate was covered with MicroAmp® 48 Well Optical Adhesive Film and centrifuged at 1000xg for 5 minutes. The plates were then placed into the StepOne™ Real-Time PCR System (Applied Biosystems, Carlsbad, CA). The default program was used; Step One: 50°C for 2 minutes, 95°C for 10 minutes; Step Two: 95°C for 15 seconds, 60°C for 1 minute, repeat 40 times.

Statistical Analysis

Statistical significance was analyzed using a one way ANOVA for the expression levels between Not Pregnant, 19 days Pregnant and 24 hours Post-Partum. A P-value of < 0.05 was considered to be significant.

Specific Aim 3: miRNA Signature of Pregnancy Induced Hypertrophy and Post-Partum Resolution

RNA Extraction

RNA extracted from Specific Aim 2 was also utilized in the completion of Specific Aim 3. RNA was diluted to 2 ng/ μ L for the cDNA reaction.

RNA conversion to cDNA (RT reaction)

For each miRNA sample, a unique cDNA reaction was completed from previously isolated total RNA. MiRNA's examined were U6 as a control, miR-1, miR-

21, miR-195 and miR-133a. Total RNA was converted to cDNA through reverse transcription for each specific miRNA sample utilizing the Taqman® MicroRNA Reverse Transcription Kit (Applied Biosystems, Carlsbad, CA). A master mix was made of the following components per reaction, as provided in the kit: 1.50 µl Reverse Transcription Buffer, 0.15 µl 100 mM dNTP Mix (with dTTP), 1.0 µl Multiscribe™ Reverse Transcriptase (50 U/µl), 4.16 µl nuclease free water and 0.19 µl RNase Inhibitor (200 U/µl). To each PCR tube, 7.0 µl of Master Mix, 3 µl primer, as specified in Table 2, and 5 µl RNA (5µg/mL) were added. The total volume of the reaction was 15 µl.

The samples were placed in a MyCycler™ Personal Thermal Cycler (Biorad, Hercules, CA). As specified in the Taqman® MicroRNA Reverse Transcription Kit protocol, the thermal cycler was set for the following program: 16°C for 30 minutes, 42°C for 30 minutes, 85°C for 5 minutes, and 4°C to hold. All RT products were placed in a -20°C freezer for storage.

Real Time PCR

A Real Time PCR reaction was completed following the cDNA reaction. All samples were done in triplicate. Master Mix was made in a 1.5 mL tube by combining the following, also accounting for the number of samples and triplicates: 1.0 µl 20x

Table 4. Primer sets utilized for miRNA Real Time PCR. All primer sets were purchased through Applied Biosystems (Carlsbad, CA). All primer sets were produced by Taqman®.

miRNA name	Applied Biosystems Assay ID	MiR Base** accession number	Mature miRNA sequence	miRNA nucleotide length
U6snRNA	001973	NR_004394*	GTGCTCGCTTCGGCAGCACATAT ACTAAAATTGGAACGATACAGA GAAGATTAGCATGGCCCCTG	55
miR-1	002222	MI0000651	CGCAAGGATGACACGCAAATTC GTGAAGCGTTCCATATTTT	22
miR-21	000397	MI0000077	UAGCUUUAUCAGACUGAUGUUGA	22
miR-133a	002246	MI0000450	UUUGGUCCCCUUAACCAAGCUG	22
miR-195	000494	MI0000489	UAGCAGCACAGAAAUAUUGGC	21
* Denotes PubMed Accession Number, not MiR Base				
** MirBase can be found at http://www.mirbase.org				

Taqman® miRNA Assays (Applied Biosystems, Carlsbad, CA), 10.0µl 2x Taqman® Gene Expression Master Mix (Applied Biosystems, Carlsbad, CA), and 7.67 µl nuclease free water. Specific primer details, including amplicon length, can be found in Table 4.

A MicroAmp® Fast Optical 48 well plate (Applied Biosystems, Carlsbad, CA) was used to run the samples. To each well, 18.67 µl Master Mix was added. For each sample, precisely 1.33 µl RT product as added into the 18.67 µl Master Mix and mixed well by pipetting up and down. The plate was covered with MicroAmp® 48 Well Optical Adhesive Film (Applied Biosystems, Carlsbad, CA) and centrifuged at 1000xg for 5 minutes. The plates were then placed into the StepOne™ Real-Time PCR System (Applied Biosystems, Carlsbad, CA). The default program was used; Step One: 50°C for 2 minutes, 95°C for 10 minutes; Step Two: 95°C for 15 seconds, 60°C for 1 minute, repeat 40 times.

Statistical Analysis

Statistical significance was analyzed using a one way ANOVA for the expression levels between Not Pregnant, 19 days Pregnant and 24 hours Post-Partum. A P-value of < 0.05 was considered to be significant.

Chapter 3

Specific Aim 1: Morphological Characterization of Pregnancy Induced Cardiac Hypertrophy and Post-Partum Cardiac Remodeling

The hypothesis for this aim is that morphology of the heart during late pregnancy will resemble the morphology of pathologic cardiac hypertrophy.

Results

A total of 25 rats were included in the study for Specific Aim 1 with a total of 18 Not Pregnant (NP), 8 Pregnant (P) and 9 Post-Pregnant (PP). For each rat the heart and body weights were recorded. Tibia lengths were recorded for n=11, n=5, and n=4 for the NP, P, and PP groups, respectively. All values are reported mean±standard deviation.

In order to determine the degree of hypertrophy, heart to body weights were analyzed. The results for the heart to body weight ratios can be found in Figure 7. The heart to body weight ratio average for the not-pregnant group was 3.92 ± 0.38 , the pregnant group 3.23 ± 0.39 , and the post-pregnant group 3.39 ± 0.88 . The heart to body weight showed a decreasing trend during pregnancy, indicative of hypertrophy, followed by a resolution post-pregnancy.

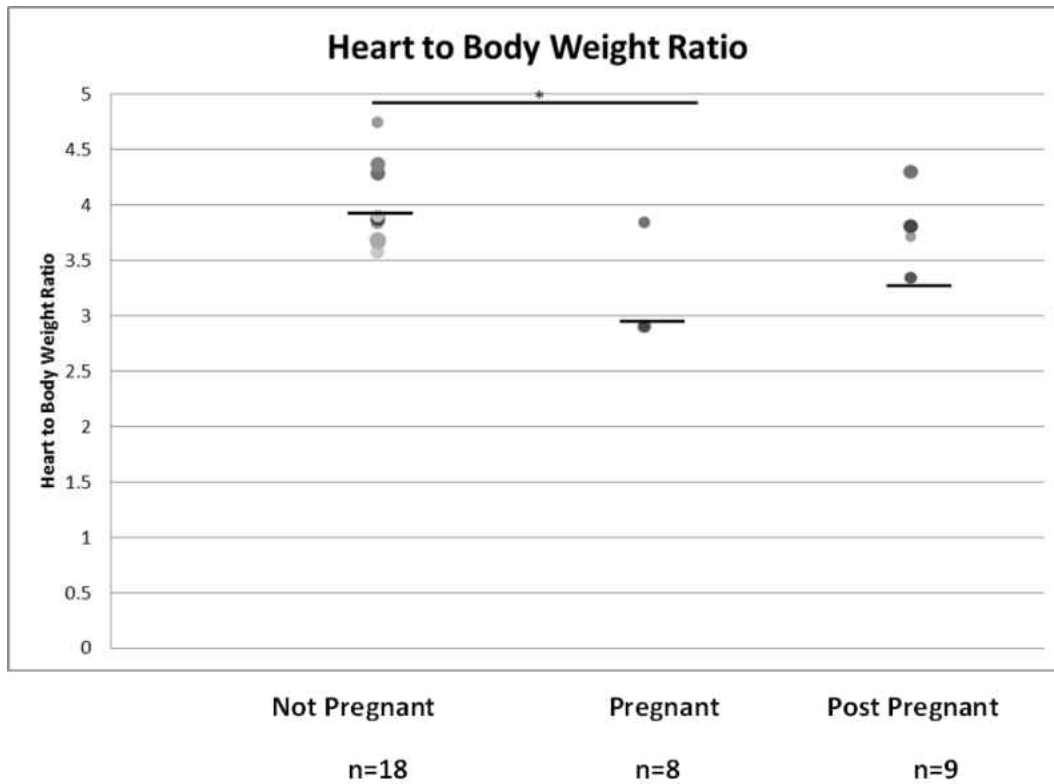


Figure 7. Heart to body weight ratios for each group. Lines denote the averages for each group, 3.92, 3.20, and 3.38 for Not Pregnant, Pregnant, and Post Pregnant, respectively. The decrease in heart to body weight ratio during pregnancy is indicative of cardiac hypertrophy, followed by a resolution post-partum. At 24 hours post-partum, the heart to body ratio increased, showing cardiac remodeling following hypertrophy. * indicates significant difference, $p < 0.05$.

The heart to tibia length ratios were: 34.02 ± 5.21 , 37.12 ± 5.61 , and 27.69 ± 1.60 , for the NP, P, and PP groups, respectively. The heart to tibia length ratios can be found in Figure 8. Results indicate hypertrophy during pregnancy with a higher heart weight to tibia length ratio.

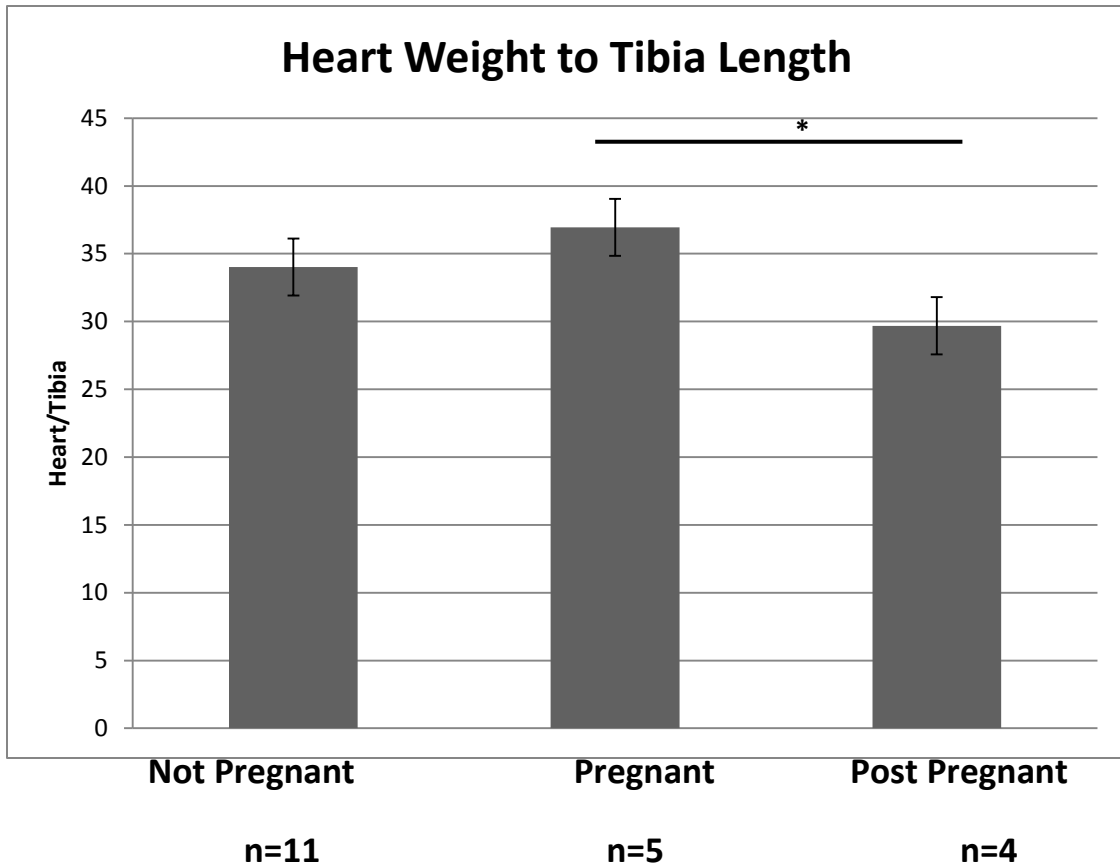


Figure 8. Heart weight (mg) to tibia length (mm) ratios for each group. The averages for each group were 34.02 ± 5.21 , 37.12 ± 5.61 , and 27.69 ± 1.60 for NP, P, and PP, respectively. As anticipated there was an increase in heart to tibia length during pregnancy followed by a decreased trend post pregnancy. * indicates significant difference, $p < 0.05$. Error bars denote standard error.

Hematoxylin & Eosin (H&E) stained slides were also prepared for analysis in Aim 1. Utilizing Nikon NIS Elements 3.2, we were able to successfully determine cardiomyocyte sizes in the NP, P and PP groups. The average cardiomyocyte sizes for the not-pregnant group were 202.03 ± 72.33 , the pregnant group 283.56 ± 139.61 , and the post-pregnant group 240.27 ± 69.88 . A schematic of the average cardiomyocyte areas can be found in Figure 9. Individual cell counts can be found in Appendix 3.

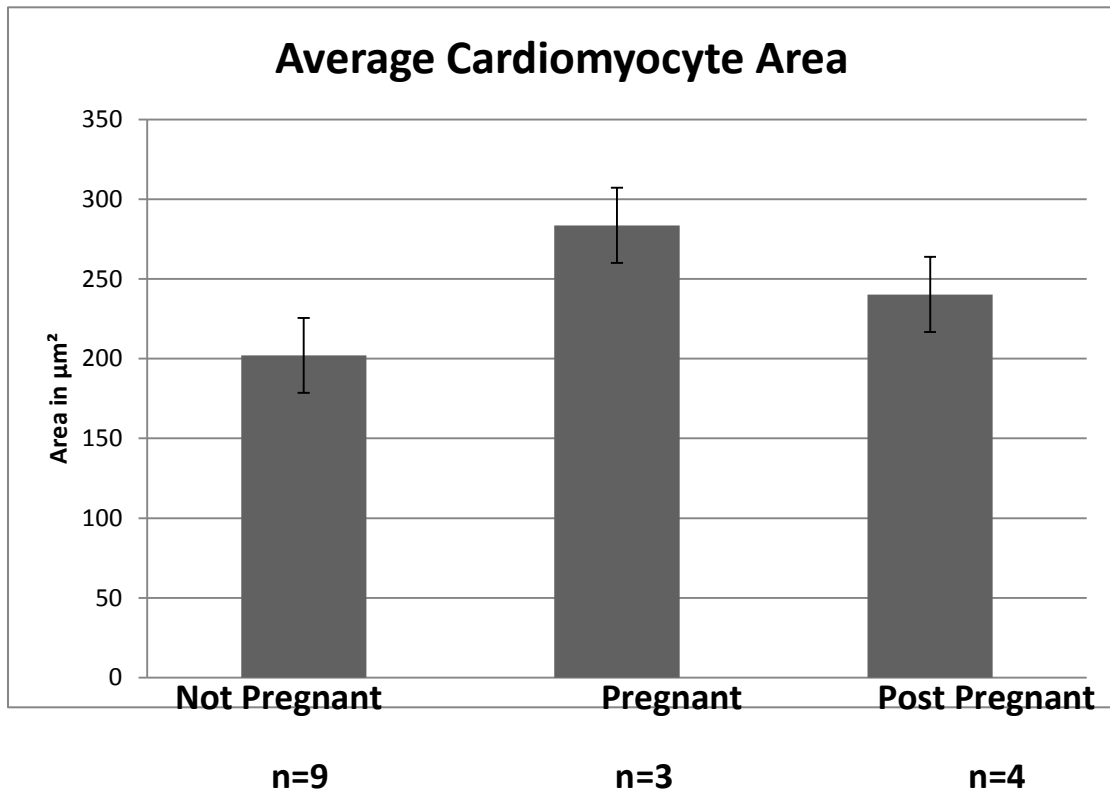


Figure 9. Cardiomyocyte areas for each group. The areas were calculated using Nikon NIS Elements 3.2. All cell sizes are in μm^2 . The averages for each group were 202.03 ± 72.33 , 283.56 ± 139.61 , and 240.27 ± 69.88 for NP, P, and PP, respectively. Cardiomyocyte size increased 40.36% during pregnancy and decreased 15.27% 24 hours post-partum. This data indicates that the cardiomyocyte areas did show hypertrophy and resolution during pregnancy and post pregnancy.. * indicates significant difference, $p < 0.05$. Error bars denote standard error.

Hematoxylin and Eosin $5 \mu\text{m}$ cross sections provided a qualitative approach to analyzing cardiac hypertrophy. Sample sizes for the hematoxylin and eosin analysis were $n=9$, $n=3$, and $n=4$ for NP, P, and PP, respectively. These cross sections showed a visual increase in thickness for the left ventricular wall as well as an increase in ventricle area. Representative images can be found in Figure 10.

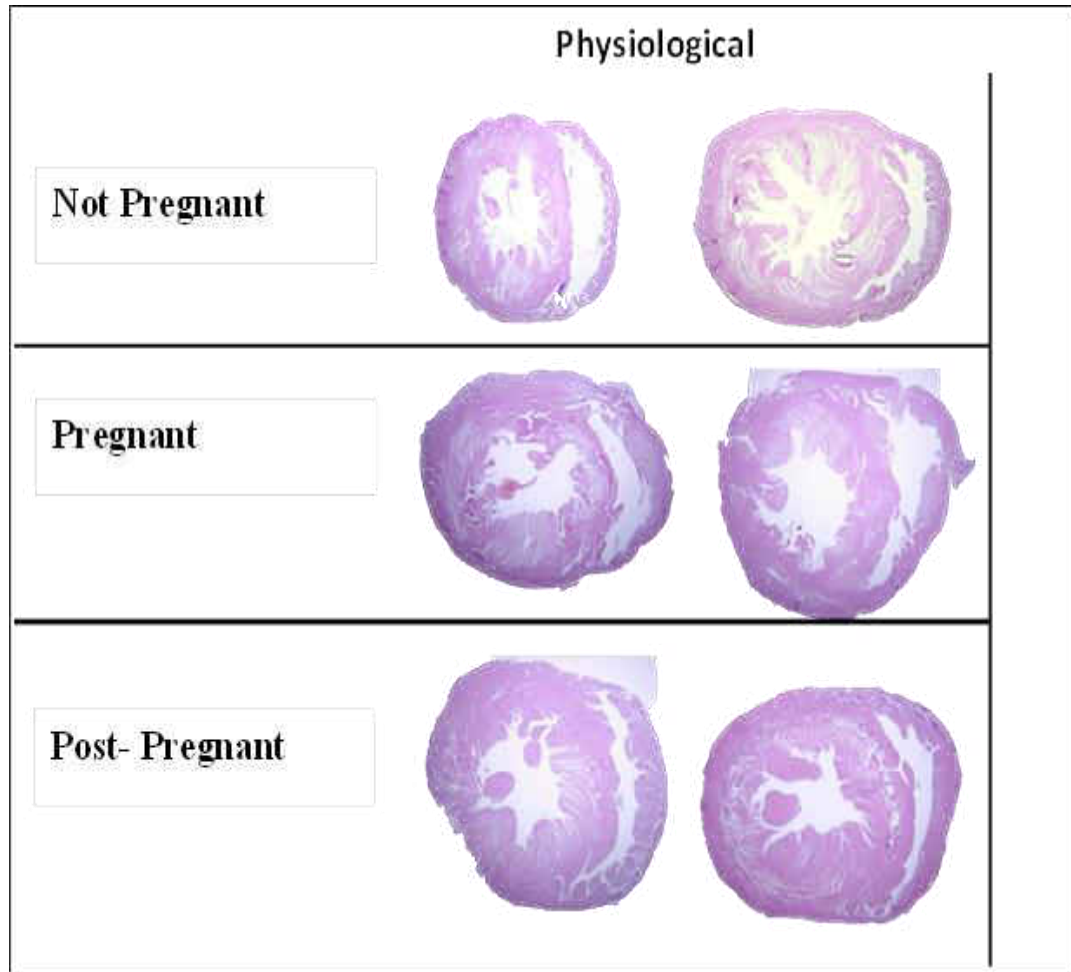


Figure 10. H&E stained 5 μ m cross section samples from each group. The Pregnant rats show relatively larger ventricles as compared to their Not Pregnant and Pregnant littermates. The Post Pregnant cross sections show a thickening of the left ventricle and a decrease in relative ventricle size.

Discussion

Cardiac hypertrophy is defined as an increase in cardiomyocyte size that can be a beneficial adaptive or a maladaptive phenomenon to compensate from stress resulting from pressure or volume overloads (Eghbali *et al.*, 2005). Prolonged hypertrophy often leads to heart failure in humans and is a major determinant of mortality and morbidity in cardiovascular diseases (Zhang, 2008). Heart failure is the leading cause of death in industrialized countries (Ahmad *et al.*, 2005; Bernardo *et al.*, 2010). Patients often do not survive one year past their diagnosis (Bultrapp *et al.*, 2005). Currently, there is a significant demand for diagnostic and/or therapeutic options for treatment and reversal of cardiac hypertrophy. If doctors are able to determine the degree of hypertrophy through simple blood tests or echocardiograms, we could potentially diagnose heart disease before it is completely irreversible.

In order to characterize pregnancy induced cardiac remodeling in rats, we first needed to establish that the rats hearts were in cardiac hypertrophy. A common method is to utilize the heart to body weight ratios. The not pregnant rats weighed an average of 272.47 ± 25.74 grams, as compared to the pregnant rats, which weighed an average of 351.23 ± 23.74 grams or an increase of 30% in body weight. Post-pregnancy the rats weighed an average of 322.6 ± 133.61 grams, or an 8% decrease from their pregnant littermates. We found a significant difference between the not-pregnant and pregnant rats when comparing body weight ($p = 0.038$).

The heart to body weight ratios provided proof that the rat's heart was indeed in cardiac hypertrophy, as the heart weights themselves increased during pregnancy. The heart weight during pregnancy increased 6% as compared to their not pregnant littermates. A lower ratio of heart to body weight was also seen during pregnancy. We found a significant difference between the not-pregnant and pregnant rats when analyzing the heart to body weight ratio ($p = 0.018$). This lower ratio signifies that both the heart increased during pregnancy, un-proportionally to the body. This finding is inconsistent with Virgen-Ortiz's report of a 15% increase in heart-to-body ratio during cardiac hypertrophy (2009). Virgen-Ortiz's research was on mice during pathological hypertrophy, demonstrating a possible difference in physiological studies. This finding is

consistent with Eghbali and colleagues, in which they found the heart to body weight ratio to be lower during pregnancy (2005).

The heart to tibia ratio was another method utilized to determine if the hearts were in hypertrophy. This technique was used in a left ventricular cardiac hypertrophy in obesity study in a mouse model by Selxas Bello Moreira *et al.* in 2009. Selxas Bello Moriera *et al.* found that in overfed mice the ratio was significantly increased as compared to their control group. This trend also correlated to the left ventricular weight, identifying another hallmark for cardiac hypertrophy. Our study found similar results, as during hypertrophy the heart to tibia ratio increased from 34.02 ± 5.21 in the not-pregnant group to 37.12 ± 5.60 in the pregnant group. We concluded a significant difference between the pregnant and post-pregnant rats' heart weight to tibia length ratio ($p=0.032$). This finding shows a similarity to previously published pathological models (Selxas Bello Moriera *et al.*, 2009).

We also examined the H&E stained cross sections to notice any visual hallmarks of cardiac hypertrophy. This technique is done frequently in mice models to show the relative sizes of each ventricle and wall thickness. Our hematoxylin and eosin cross sections identified a larger left ventricle and thicker ventricular walls. This finding is consistent with previous physiological findings, as eccentric hypertrophy results in chamber enlargement, considered to be a proportional change to the left ventricular wall thickness (McMullen & Jennings, 2007). This data is comparable to pathological hypertrophy, where the chamber walls thicken un-proportionally to the left ventricle chamber (McMullen & Jennings, 2007). While this method might be of use for pathological hypertrophy studies, the changes are not distinct enough for distinguishing physiological hypertrophy. It is rather difficult to notice the chamber sizes relative to one another. Future studies should utilize an echocardiogram to determine wall thickness.

The H&E stained cross sections were then examined under a microscope for changes in cardiac myocyte sizes. During both pathological and physiological cardiac hypertrophy, the myocytes enlarge to alleviate pressure and volume overloads (Bultrago *et al.*, 2005). While the heart remodels itself back to normal post-pregnancy, we

anticipated that the cardiomyocyte cell sizes decrease back to their original not-pregnant littermates myocyte sizes. The average cardiomyocyte area for the not-pregnant group was $202.03 \pm 72.33 \mu\text{m}^2$, pregnant $283.56 \pm 139.61 \mu\text{m}^2$, and post pregnant $240.27 \pm 69.05 \mu\text{m}^2$. This data supports the hypothesis that the myocyte size does alter following pressure and volume overloads. The post-pregnant data indicates that even at 24 hours post-partum the heart is already remodeling itself back towards pre-pregnancy. We did not conclude a significant difference between the three groups' cardiomyocyte areas.

In specific aim 1 our goal was to identify morphological characteristics of pregnancy induced cardiac hypertrophy and post-partum remodeling. We hypothesized that the morphological characterization during late pregnancy was to resemble the morphological changes during pathological hypertrophy. Through analyzing different components of data, such as the heart to body ratio and heart to tibia ratio, we determined that during pregnancy, the rat's hearts were indeed in cardiac hypertrophy. Several components of our data showed dissimilarities to pathological hypertrophy. The heart to body ratio was lower when compared to previous pathological studies. As anticipated, the H&E stained cross sections showed dissimilarities in wall and chamber thickness. The cardiomyocyte area sizes were similar to pathological studies and should continue to be used in future studies.

Chapter 4

Specific Aim 2: Biochemical Characterization of Pregnancy Induced Cardiac Hypertrophy and Post-Partum Cardiac Remodeling

The hypothesis for this aim was that known pathological cardiac hypertrophy genes will also be expressed in rat pregnancy induced cardiac hypertrophy and expression will be lost during post-partum remodeling.

Results

A total of 14 rats were used in the Real Time analysis portion of Specific Aim 2; n=5 not-pregnant (NP), n=4 pregnant (P) and n=5 post-pregnant (PP). The control for genetic expression Real Time PCR used was GAPDH. Information regarding primers for Real Time PCR can be found in Table 3. A schematic of all the results in Aim 2 can be found in Figure 11.

The myosin heavy chain protein, α -MHC, is a cardiac specific sarcomeric gene highly expressed in the atrial septum (Posch *et al.*, 2010). A recent study done by Malik and colleagues emphasized the potential for α -MHC to be utilized as a therapeutic target during cardiac hypertrophy (Malik *et al.*, 2011). The gene expression analysis for α -MHC showed an increasing trend, from 1.49 ± 0.91 fold expression in not pregnant rats to 2.74 ± 3.18 fold expression in pregnant rats, and 2.36 ± 1.78 in post-pregnant rats. This is in contrast to what is usually seen in pathological cardiac hypertrophy.

G-protein estrogen receptor, GPER, can mediate estrogen induced non-genomic signaling events, such as activation of the MAPK and PI3K pathways (Ariazi *et al.*, 2010). GPER has not been previously studied in pathological or physiological cardiac hypertrophy. GPER expression increased during pregnancy but then returned back to their NP littermates during post-pregnancy; with 0.87 ± 0.55 for not-pregnant, 2.33 ± 3.09 for pregnant, and 1.05 ± 0.84 for post-pregnant rats.

The natriuretic peptides, such as ANP and BNP, are internally derived antagonists that are important in metabolic regulation and cardiovascular remodeling (Savoia *et al.*, 2010). Previous studies have demonstrated that ANP and BNP typically increase during

the onset of pathologic hypertrophy (Savoia *et al.*, 2010). During pregnancy induced cardiac hypertrophy, atrial natriuretic peptide (ANP) instead decreased in expression. Expression levels for ANP were 1.46 ± 0.93 for not-pregnant, 0.41 ± 0.31 for pregnant, and 0.48 ± 0.44 for post pregnant. B-type natriuretic peptide remained the same even throughout pregnancy and post-pregnancy. The values for BNP are 1.16 ± 1.16 for not pregnant, 1.27 ± 1.14 for pregnant, and 1.74 ± 1.54 for post pregnant rats.

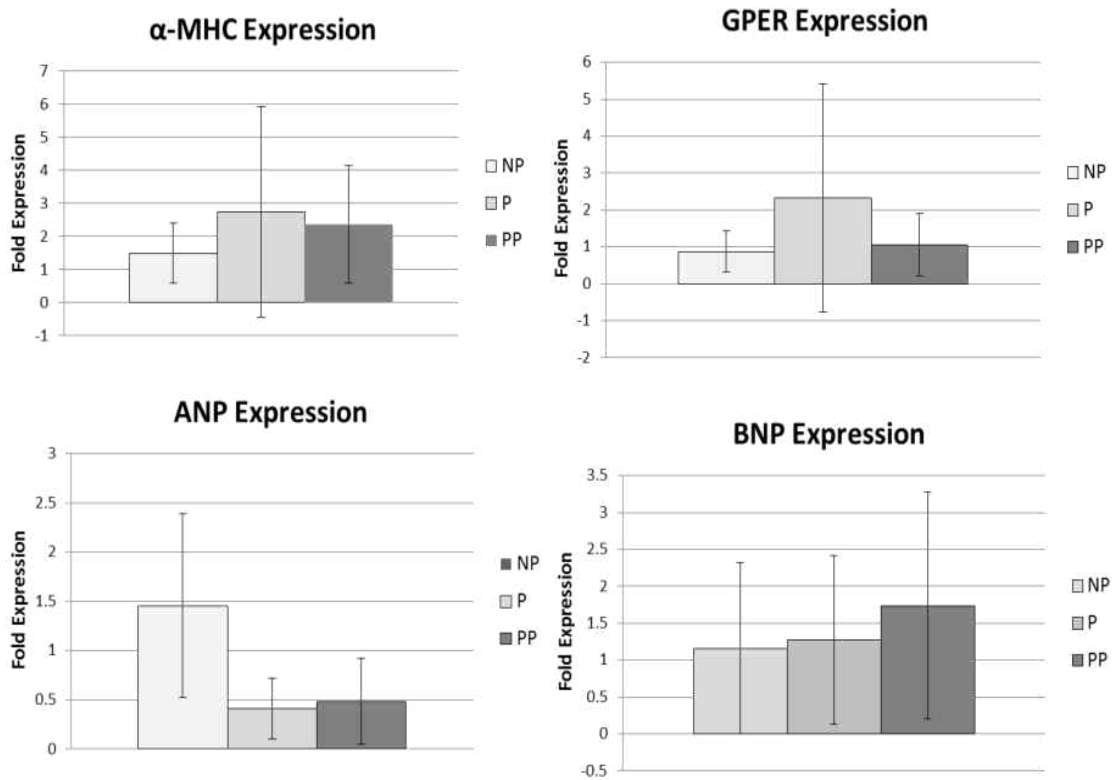


Figure 11. Expression levels for each α -MHC, GPER, ANP, and BNP. Samples were not pregnant (NP), 19 days pregnant (P), and 24 hours post-partum (PP). α -MHC showed increasing levels of expression during pregnancy, unlike what has been seen in pathological cardiac hypertrophy. GPER has yet to be studied in physiological hypertrophy, and showed increased levels during pregnancy followed by a full resolution post-pregnancy. ANP, up-regulated during pathological hypertrophy, was down-regulated during pregnancy and post pregnancy. BNP is up-regulated during pathological hypertrophy and showed no change during physiological hypertrophy. Error bars denote standard error.

Discussion

Gene expression markers, such as atrial natriuretic peptide (ANP), B-type natriuretic peptide (BNP) and alpha myosin heavy chain (α -MHC) have all been studied during pathological and physiological cardiac hypertrophy. While studies have been conducted in mice to determine the expression of hypertrophy markers during pregnancy induced cardiac hypertrophy, changes in expression during post-partum cardiac remodeling (resolution of hypertrophy) have not been characterized. Since we used a rat model, we were the first to document hypertrophy marker expression in pregnancy induced hypertrophy.

Alpha myosin heavy chain is a cardiac specific sarcomeric gene highly expressed in the atrial septum (Posch *et al.*, 2010). An increase in β -MHC expression and a decrease in α -MHC expression have been accepted as cardiac hypertrophy markers for the past 40 years (Barry *et al.*, 2008). The cardiac remodeling process following hypertrophy is generally associated with the return of the MHC isoforms back to normal (Barry *et al.*, 2008). Our study demonstrated similar non-significant findings of this current standard; as α -MHC levels increased during pregnancy and decreased slightly during post-pregnancy. There are a few reasons why this result occurred. First, α -MHC is the primary MHC isoform in rodents (Barry *et al.*, 2008). In order to get a clearer picture of the genetic expression during pregnancy, studying β -MHC would be beneficial to determine the ratio between the two isoforms. Perhaps, in rats, α -MHC plays a protective role during pregnancy, contrary to previous studies. Future studies should also connect the role of estrogen and α -MHC to see if both exert a protective effect during hypertrophy.

GPER, or G Protein Coupled Estrogen Receptor, has never been analyzed during pregnancy induced cardiac hypertrophy in rats. GPER can mediate estrogen induced non-genomic signaling events, such as activation of the MAPK and PI3K pathways (Ariazi *et al.*, 2010). Our results show that during cardiac hypertrophy, GPER is highly expressed, followed by a decrease in expression post-pregnancy. This result correlates

with the higher levels of expression in estrogen during pregnancy. Higher levels of estrogen mean that higher amounts are binding to GPER to initiate signaling pathways.

The natriuretic peptides, ANP and BNP, showed both elevated and decrease levels of expression during pregnancy and 24 hours post-partum. These peptides are internally derived antagonists of vasoconstriction that are important during cardiac remodeling (Savoia *et al.*, 2010). During pathological hypertrophy, both ANP and BNP are considered to be up-regulated (Bernardo *et al.*, 2010). In our study, the expression of ANP is contradictory to previously published pathological studies (Savoia *et al.*, 2010). ANP is an inhibitor of renin, which mediates extracellular volume of blood, lymph, and interstitial fluid (Savoia *et al.*, 2010). During pregnancy, perhaps ANP is down-regulated due to the connection with renin, as it is possible that renin is necessary during pregnancy due to the increased volume of blood throughout the body and placenta. The sample size for this study was rather small, and a clear difference in expression levels might become clearer following a larger study.

The working hypothesis for this aim was that known pathological cardiac hypertrophic genes will also be expressed in rat pregnancy induced cardiac hypertrophy and expression will be lost during post-partum remodeling. Analysis of genetic markers, such as α -MHC, GPER, ANP and BNP indicate that physiological hypertrophy shares similarities and differences with pathological hypertrophy. For example, α -MHC showed higher expression levels during pregnancy and post-pregnancy during physiological hypertrophy but lower expression during pathological hypertrophy. GPER, never studied previously in physiological hypertrophy, showed higher levels of expression during pregnancy. ANP, up-regulated during pathological hypertrophy was down-regulated during pregnancy and post-pregnancy. BNP, also up-regulated during pathological hypertrophy, showed no changes in expression during pregnancy induced cardiac hypertrophy and 24 hours post-pregnancy, contrary to what has been seen before.

Chapter 5

Specific Aim 3: MiRNA signature of Pregnancy Induced Hypertrophy and Post-Partum Resolution

The hypotheses for this aim were; (1) miRNA expression patterns during cardiac hypertrophy will be similar to that of pathological hypertrophy and (2) miRNA expression patterns in the post-partum heart will be similar to the normal heart.

Results

Four separate miRNA's were analyzed in this study; miR-1, miR-133a, miR-21 and miR-195. All miRNA reagents and control information can be found in Table 4. Sample sizes were: n=3 for not pregnant (NP), n=5 for pregnant (P), and n=5 for post pregnant (PP). A schematic with the results for this aim can be found in Figure 12.

MiR-1 is down-regulated during pathological hypertrophy. During pregnancy induced cardiac hypertrophy, we found the expression levels to be as follows: 1.09 ± 0.43 for not pregnant, 2.41 ± 2.54 for pregnant, and 2.36 ± 1.78 for post pregnant. Expression levels increased slightly during pregnancy and further increased during post-pregnancy. Mir-133a is also down-regulated during pathological hypertrophy. We found expression levels for miR-133a to be the following; 1.45 ± 1.68 for not pregnant, 4.26 ± 1.45 for pregnant, and 2.87 ± 1.81 for post-pregnant. Expression levels, similar to miR-1, increased during pregnancy and further increased during post-pregnancy.

Both miR-195 and miR-21 are up-regulated during pathological cardiac hypertrophy (*van Rooij et al.*, 2008). We found similar results for our study. MiR-21 expression was as follows; 1.70 ± 2.42 for not pregnant, 10.25 ± 10.16 pregnant and 7.11 ± 4.69 for post pregnant. MiR-195 followed a similar pattern; 1.96 ± 2.67 for not pregnant, 8.53 ± 6.44 for pregnant, and 3.45 ± 3.58 for post pregnant. These expression levels mimic those seen in pathological cardiac hypertrophy.

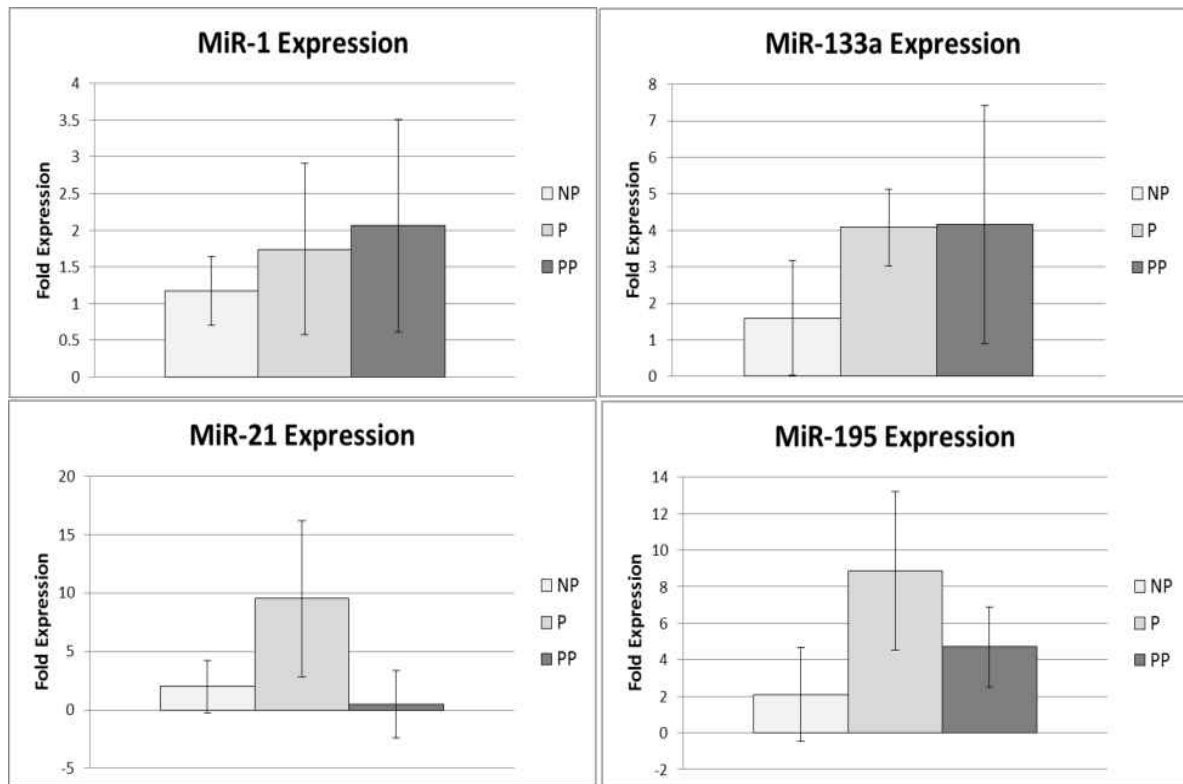


Figure 12. Expression levels for miR-1, miR-133a, miR-21 and miR-195. Samples were not pregnant (NP), 19 days pregnant (P), and 24 hours post-partum (PP). MiRNAs 1 and 133a are usually seen to be down-regulated during pathological hypertrophy, but are slightly up-regulated in our study. MiR-21 and 195 are both up-regulated during pregnancy, and our study showed similar results. Error bars denote standard error.

Discussion

MicroRNA's are short, endogenous, non-coding single stranded segments of RNA that regulate gene expression through hybridization to messenger RNA (Zhang, 2011). The terminal consequence of miRNA binding to mRNA could be either mRNA degradation or inhibition of translated targets (Zhang, 2011). MiRNAs have become of great attention lately because of their importance in cardiovascular development, vascular angiogenesis, hypertrophy, and cardiovascular diseases (Shen *et al.*, 2010). MiRNAs such as miR-21, miR-195, miR-133 and miR-208 all play a role in the process of cardiac remodeling by regulating changes in gene expression that accompany pathological disorders (Sucharov *et al.*, 2008). In this study, we focused on miR-1, miR-133a, miR-21, and miR-195 and their connection to pregnancy induced physiological cardiac hypertrophy.

MiRNA-1 and miRNA-133a are derived from the same precursor and are both said to be down-regulated during pathological cardiac hypertrophy (van Rooij *et al.*, 2008). MiRNA-1 is considered pro-apoptotic and excess of miR-1 leads to a decreased pool of proliferating cardiomyocytes (Mishra *et al.*, 2009). MiR-1 is transcriptionally regulated by myogenic differentiation factors, such as MyoD, Mef2, and SRF (Zorio *et al.*, 2009). SRF is a transcription factor that recruits co-activators and myocardin to muscle specific genes that control differentiation (Callis *et al.*, 2009; Zhang, Ashar, Helms & Wei, 2011). In our study, we found miR-1 to be up-regulated during pregnancy induced cardiac hypertrophy, although no significant difference was identified. Perhaps expression of miR-1 is necessary for proper fetal development due to SRF levels. We found miRNA-133a to also be up-regulated. Several of miRNA-133a's targets include HCN2, Cdc42, and RhoA (Luo *et al.*, 2008; Bauersachs & Thum, 2007). MiRNA-133a also suppresses SRF. SRF appears to play a role during cardiac hypertrophy and resolution. More studies need to be conducted to determine both miR-1 and miR-133a expression during pregnancy induced cardiac hypertrophy as well as their connection to SRF.

In our experiments, miR-195 was highly up-regulated as compared to their not-pregnant littermates. MiR-195's targets have yet to be identified; however, up-regulation

of miR-195 in transgenic models resulted in dilated cardiomyopathy and heart failure in mice as early as 2 weeks old (van Rooij *et al.*, 2008). Another study by Shen *et al.* in 2010 provided similar results; as miR-195 over-expression lead to heart failure in mice. MiR-195's expression pattern during physiological cardiac hypertrophy is similar to pathological cardiac hypertrophy.

MiR-21 is involved in tumor-related cell growth and apoptosis, mediation of signaling pathways in neonatal cardiomyocytes, along with much more (Shen *et al.*, 2010). The exact molecular target of miR-21 have yet to be identified; however, knockout models suggest that SPRY1 is targeted, a potential inhibitor of the RAS/MEK/ERK pathway (Thum *et al.*, 2008). Similar to what is seen in pathological hypertrophy studies, we saw an increase in miR-21's expression during hypertrophy followed by a drop in expression 24 hours post-partum. The drastic drop 24 hours post-partum could be an indicator of the healthy remodeling process. The high levels of miR-21 most likely correlate to the inhibition of the RAS/MEK/ERK pathway (Thum *et al.*, 2008). This pathway is often found in cancer cells, as it controls transcription and translation of these cells. Once miR-21 inhibits the RAS pathway, transcription and translation of cells is halted, thus probably altering cell proliferation and apoptosis.

By looking at the relationships of miR-1, miR-133a, miR-195, and miR-21 during physiological hypertrophy, we are able to relate them to pathological cardiac hypertrophy. We found higher levels of expression of miR-1 and miR-133a during physiological hypertrophy, contrary to pathological studies. We found increased levels of expression for miR-21 and miR-195 during physiological cardiac hypertrophy which mimics that of pathological cardiac hypertrophy.

Chapter 6

Summary and Future Directions

The overarching purpose of this study was to characterize physiological hypertrophy and relate it to pathological hypertrophy. Through a series of experiments, we were successfully able to analyze different components of cardiac hypertrophy during pregnancy. From there, we were then able to compare and contrast our results with that of pathological hypertrophy.

In specific aim 1, we looked at heart weights, body weights, and tibia lengths to determine if the rat's hearts were hypertrophied. We saw an increase in heart and body weights, and thus assumed the hearts were in hypertrophy. H&E cross sections showed the ventricle walls and chambers; however, this method was not reliable for determining the degree of hypertrophy. Looking at the H&E slides, we saw that in physiological hypertrophy, the wall thickens proportionally the chambers; while in pathological hypertrophy the walls become thin and chambers enlarge. More studies should include an echocardiogram to quantitatively determine left ventricular sizes. The echocardiogram would provide another approach to quantitatively distinguish cardiac hypertrophy. From the H&E slides we looked at the individual cardiomyocytes in each of the not pregnant, pregnant and post pregnant. We saw an increase in cardiomyocyte cell sizes during pregnancy followed by a decrease in cell sizes post pregnancy. Utilizing paraffin embedded slides, it might be of use to use immunofluorescence as another method to qualitatively visualize cellular expression during hypertrophy. Atrial natriuretic factor and α -actinin would be two cellular markers of use to analyze in future studies.

In specific aim 2, we used Real Time PCR to analyze gene expression during pregnancy. Our results were varied and dissimilar with what has been seen in pathological hypertrophy. Alpha myosin heavy chain was increased during pregnancy, while in pathological hypertrophy expression is decreased. Future studies should consider analyzing β -MHC expression as well as α -MHC, as the two isoforms are usually present in any tissue sample. GPER was also analyzed for the first time in our

physiological cardiac hypertrophy study. GPER expression increased during pregnancy and decreased 24 hours post-partum. Estrogen levels also increase during pregnancy, explaining the importance of estrogen during pregnancy. Future studies could look at the other two estrogen receptors, ER- α and ER- β , to determine the relationship between the three receptors during pregnancy induced cardiac hypertrophy. The natriuretic peptides were also studied in specific aim 2. An increased level of expression for both ANP and BNP has been a hallmark of pathological cardiac hypertrophy for many years. In our study ANP decreased during physiological hypertrophy. BNP, on the other hand, showed no change in expression during pregnancy or post pregnancy. Perhaps to get a better picture of these natriuretic peptides, one should look into the precursors, pro-ANP and pro-BNP. These precursors are much more stable than their active counterparts, and might produce more accurate data.

In specific aim 3, we looked at miRNA expression using Real Time PCR. We saw that miR-1 and miR-133a both increased slightly during pregnancy, contradictory to what is seen in pathological cardiac hypertrophy. MiR-21 and miR-195 both increased during pregnancy, which mimics what is seen during pathological cardiac hypertrophy. In order to produce statistically significant results, it would be beneficial to repeat the expression analysis on a larger sample size. This might provide a clearer idea regarding the significance of miR-1 and miR-133a during physiological cardiac hypertrophy. Another possibility would be to examine the known miRNA targets. For miR-1 and miR-133a, analysis of SRF during hypertrophy and for miR-21, analysis of SPRY1.

Therapeutic applications to our miRNA and gene expression experiments are possible within the near future. Gene therapy, especially with those genes discussed in our research, could be used as a method to remediate cardiac hypertrophy. Targeting the myosin heavy chain through omecamtiv mecarbil treatment could increase cardiac function without changing the rate of contractions. Gene expression testing for hypertrophy markers such as ANP or BNP or their precursors could identify a hypertrophy problem that has yet to show symptoms. As demonstrated in our GPER results, estrogen does play a role during cardiac hypertrophy. A simple estrogen hormone treatment could remediate a woman with prolonged cardiac hypertrophy. Using

a GPER agonist such as G-1, which halts cell cycle progression, could be utilized as a cancer treatment to stop uncontrollable proliferation.

Through targeting specific miRNA, such as miR-1 and miR-133a, we could be able to increase expression and thus halt cardiac hypertrophy. Offering patients a medication with a miRNA antagonist, similar to what has already been tested in the laboratory, could provoke cardiac remodeling during hypertrophy.

During pregnancy, a woman's heart enlarges to compensate for added stress and volume overloads. Following delivery, most women's hearts return back to their pre-pregnancy size. For a small percentage of women, however, their hearts are unable to remodel themselves back to normal, thus increasing their chances of heart failure. Our research and others have demonstrated changes in miRNA and gene expression during pregnancy. MicroRNAs have recently been detected in the blood. Pregnant women could be given a simple blood test to determine their risk for developing pathological hypertrophy. If these women test positive, an early diagnosis as well as treatment could save many women from becoming a statistic.

References

- Ahmad, F., Seidman, J.G. and Seidman, C.E. (2005). The genetic basis of cardiac remodeling. *Annu. Rev. Genomics Hum. Genet.*, 6, 185-216.
- Akashi, Y.J., Springer, J., Lainscak, M. and Anker, S.D. (2007). Atrial natriuretic peptide and related peptides. *Clin. Chem. Lab. Med.*, 45, 1259-1267.
- Ariazi, E.A., Brailoiu, E., Yerrum, S., Shupp, H.A., Slifker, M.J., Cunliffe, H.E., Black, M.A., Donato, A.L., Arterburn, J.B., Oprea, T.I., Prossnitz, E.R., Dun, N.J. and Jordan, V.C. (2010). The G protein coupled receptor GPR30 inhibits proliferation of estrogen receptor-positive breast cancer cells. *Cancer Res.*, 70, 1184-1194.
- Balakumar, P. and Singh, M. (2006). Differential role of rho-kinase in pathological and physiological cardiac hypertrophy in rats. *Pharmacology*, 78, 91-97.
- Barrick, C.J., Dong, A., Waikel, R., Corn, D., Yang, F., Threadgill, D.W. and Smyth, S.S. (2009). Parent-of-origin effects on cardiac response to pressure overload in mice. *Am J Physiol. Heart Circ. Physiol.*, 297, 1003-1009.
- Barry, S.P., Davidson, S.M., Townsend, P.A. (2008). Molecular regulation of cardiac hypertrophy. *The Int. J. Biochem. Cell Biol.*, 40, 2023-2039.
- Bauersachs, J. and Thum, T. (2007). MicroRNAs in the broken heart. *Eur. J. Clin. Invest.*, 37, 829-833.
- Bernardo, B.C., Weeks, K.L., Pretorius, L. and McMullen, J.R. (2010). Molecular distinction between physiological and pathological cardiac hypertrophy: experimental findings and therapeutic subjects. *Pharmacol. Ther.*, 128, 191-227.
- Boštjančič, E., Zidar, N., Štajer, D. and Glavač, D. (2010). MicroRNAs miR-1, miR-133a, miR-133b and miR-208 are dysregulated in human myocardial infarction. *Cardiology*, 115, 163-169.
- Buitrago, M., Lorenz, K., Maass, A.H., Oberdorf-Maass, S., Keller, U., Schmitteckert, E.M., Ivaschchenko, Y., Lohse, M.J. and Engelhardt, S. (2005). The transcriptional repressor Nab1 is a specific regulator of pathological cardiac hypertrophy. *Nature Med.*, 11, 837- 844.
- Busk, P.K. and Cirera, S. (2010). MicroRNA profiling in early hypertrophic growth of the left ventricle in rats. *Biochem. Biophys. Res. Commun.*, 396, 989-993.
- Cai, B.Z., Pan, Z.W. and Lu, Y.J. (2010). The roles of microRNAs in heart diseases: a novel important regulator. *Curr. Med. Chem.*, 17, 407-411.

- Callis, T.E., Chen, J. and Wang, D. (2007). MicroRNAs in Skeletal and Muscle Development. *DNA Cell Biol.*, 26, 219-225.
- Callis, T.E., Pandya, K., Seok, H.Y., Tang, R., Tatsuguchi, M., Huang, Z., Chen, J., Deng, Z., Gunn, B., Shumate, J., Willis, M.S., Selzman, C.H. and Wang, D. (2009). MicroRNA-208a is a regulator of cardiac hypertrophy and conduction in mice. *J. Clin. Invest.*, 119, 2772-2786.
- Callis, T.E. and Wang, D. (2008). Taking microRNAs to heart. *Trends Mol. Med.*, 14, 254-260.
- Carè, A., Catalucci, D., Felicetti, F., Bonci, D., Addario, A., Gallo, P., Bang, M., Segnalini, P., Gu, Y., Dalton, N.D., Elia, L., Latronico, M.V.G., Høydal, M., Autore, C., Russo, M.A., Dorn, G.W., Ellingsen, Ø., Ruiz-Lozano, P., Peterson, K.L., Croce, C.M., Peschle, C. and Condorelli, G. (2007). MicroRNA-133 controls cardiac hypertrophy. *Nature Med.*, 13, 613-618.
- Catalucci, D., Latronico, M.V.G., Ellingsen, O. and Condorelli, G. (2008). Physiological myocardial hypertrophy: how and why?. *Front. Biosci.*, 13, 312-324.
- Chen, J., Murchison, E.P., Tang, R., Callis, T.E., Tatsuguchi, M., Deng, Z., Rojas, M., Hammond, S.M., Schneider, M.D., Selzman, C.H., Meissner, G., Patterson, C., Hannon, G.J. and Wang, D. (2007). Targeted deletion of dicer in the heart leads to dilated cardiomyopathy and heart failure. *PNAS*, 105, 2111-2116.
- Ching, Y., Ghosh, T.K., Cross, S.J, Packham, E.A., Honeyman, L., Loughna, S., Robinson, T.E., Dearlove, A.M., Ribas, G., Bonser, A.J., Thomas, N.R., Scotter, A.J., Caves, L.S.D., Tyrrell, G.P., Newbury-Ecob, R.A., Munnich, A., Bonnet, D. and Brook, J.D. (2005). Mutation in myosin heavy chain 6 causes atrial septum defect. *Nature Genet.*, 37, 423-428.
- Dennis, M.K., Burai, R., Ramesh, C., Petrie, W.K., Alcon, S.N., Nayak, T.K., Bologna, C.G., Leitao, A., Brailoiu, E., Deliu, E., Dun, N.J., Sklar, L.A., Hathaway, H.J., Arterburn, J.B., Oprea, T.I. and Prossnitz, E.R. (2009). *In vivo* effects of a GPR30 antagonist. *Nat. Chem. Biol.*, 6, 421-427.
- Deschamps, A.M. and Murphy, E. (2009). Activation of a novel estrogen receptor, GPER, is cardioprotective in male and female rats. *Am. J. Physiol. Heart Circ. Physiol.*, 297, H1806-H1813.
- Eghbali, M., Deva, R., Alioua, A., Minosyan, T.Y., Ruan, H., Wang, Y., Toro, L. and Stefani, E. (2005). Molecular and functional signature of heart hypertrophy during pregnancy. *Circ. Res.*, 96, 1208-1216.

- Engle, S.K., Solter, P.F., Credille, K.M., Bull, C.M., Adams, S., Berna, M.J., Schultze A.E., Rothstein, E.C., Cockman, M.D., Pritt, M.L., Liu, H., Lu, Y., Chiang, A.Y. and Watson, D.E. (2010). Detection of left ventricular hypertrophy in rats administered a peroxisome proliferator-activated receptor α/γ dual agonist using natriuretic peptides and imaging. *Toxicol. Sci.*, 114, 183-192.
- Foryst-Ludwig, A., Kreissl, M.C., Sprang, C., Thalke, B., Böhm, C., Benz, V., Gürgen, D., Dragun, D., Schubert, C., Mai, K., Stawowy, P., Spranger, J., Regitz-Zagrosek, V., Unger, T. and Kintscher, U. (2011). Sex differences in physiological cardiac hypertrophy are associated with exercise-mediated changes in energy substrate availability. *Am. J. Physiol. Heart Circ. Physiol.*, in press.
- Friedman, R.C., Kai-How Farh, Burge, C.B. and Bartel, D.P. 2010. Most mammalian mRNAs are conserved targets of microRNAs. *Genome Res.*, 19, 92-105.
- Granados-Riveron, J.T., Ghosh, T.K., Pope, M., Bu'Lock, F., Thornborough, C., Eason, J., Kirk, E.P., Fatkin, D., Feneley, M.P., Harvey, R.P., Armour, J.A.L. and J.D. Brook. (2010). α -cardiac myosin heavy chain (MYH6) mutations affecting myofibril formation are associated with congenital heart defects. *Hum. Mol. Gen.*, 19, 4007-4016.
- Haghikia, A. and Hilfiker-Kleiner, D. (2009). MiRNA-21: a key to controlling the cardiac fibroblast compartment? *Cardiovasc. Res.*, 82, 1-3.
- Hildebrandt, P. (2009). Natriuretic peptides: prediction of cardiovascular disease in the general population and high risk populations. *Dis. Markers*, 26, 227-233.
- Iemitsu, M., Maeda, S., Miyauchi, T., Matsuda, M. and Tanaka, H. (2005). Gene expression profiling of exercise-induced cardiac hypertrophy in rats. *Acta. Physiol. Scandinavica*, 185, 259-270.
- Jacob, H.J. and Kwitek, A.E. (2002). Rat genetics: attaching physiology and pharmacology to the genome. *Nature*, 3, 33-42.
- Kasama, S., Furuya, M, Toyama, T., Ichikawa, S. and Kurabayashi, M. (2008). Effect of atrial natriuretic peptide on left ventricular remodeling in patients with acute myocardial infarction. *Eur. Heart J.*, 29, 1485-1494.
- Lagos-Quintana, M., Rauhut, R., Meyer, J., Borkhardt, A. and Tuschl, T. (2003). New microRNAs from mouse and human. *RNA*, 9, 175-179.
- Latronico, M.V.G., Catalucci, D. and Condorelli, G. (2008). MicroRNA and cardiac pathologies. *Physiol. Genomics*, 34, 239-242.

- Li, Q., Song, X., Zou, J., Wang, G., Kremneva, E., Li, X., Zhu, N., Lappalainen, P., Yuan, W., Qin, Y. and Jing, Q. (2010). Attenuation of microRNA-1 derepresses the cytoskeleton regulatory protein twinfilin-1 to provoke cardiac hypertrophy. *J. Cell Sci.*, 123, 2444-2452.
- Luo, X., Lin, H., Pan, Z., Xiao, J., Zhang, Y., Lu, Y., Yang, B. and Wang, Z. (2008). Down-regulation of miR-1/miR-133 contributes to re-expression of pacemaker channel genes HCN2 and HCN4 in hypertrophic heart. *J. Biol. Chem.*, 283, 20045-20052.
- Magnusson, M., Jovinge, S., Rydberg, E., Dahlöf, B., Hall, C., Nielsen, O.W., Grubb, A. and Willenheimer, R. (2009). Natriuretic peptides as indicators of cardiac remodeling in hypertensive patients. *Blood Press.*, 18, 196-203.
- Malik, F.I., Hartman, J.J., Elias, K.A., Morgan, B.P., Rodriguez, H., Brejc, K., Anderson, R.L., Sueoka, S.H., Lee, K.H., Finer, J.T., Sakowicz, R., Baliga, R., Cox, D.R., Garard, M., Godinez, G., Kawas, R., Kraynack, E., Lenzi, D., Lu, P.P., Muci, A., Niu, C., Qian, X., Pierce, D.W., Pokrovskii, M., Suehiro, I., Sylvester, S., Tochimoto, T., Valdez, C., Wang, W., Katori, T., Kass, D.A., Shen, Y., Vatner, S.F. and Morgans, D.J. (2011). Cardiac myosin activation: a potential therapeutic approach for systolic heart failure. *Science*, 331, 1439-1443.
- McMullen, J.R. and Jennings, G.L. (2007). Differences between pathological and physiological cardiac hypertrophy: novel therapeutic strategies to treat heart failure. *Clin. Exp. Pharmacol. Physiol.*, 34, 255-262.
- Mishra, P.K., Tyagi, N., Kumar, M. and Tyagi, S.C. (2009). MicroRNAs as a therapeutic target for cardiovascular diseases. *J. Cell. Mol. Med.*, 13, 778-789.
- Mizukami, Y. (2010). *In vivo* functions of GPR30/GPER-1, a membrane receptor for estrogen: from discovery to functions *in vivo*. *Endocrine Journal*, 57, 101-107.
- Moertl, D., Berger, R., Struck, J., Gleiss, A., Hammer, A., Morgenthaler, N.G., Bergmann, A., Huelsmann, M. and Pacher, R. (2009). Comparison of midregional pro-atrial and B-type natriuretic peptides in chronic heart failure. *J. Am. Coll. Cardiol.*, 53, 1783-1790.
- Patrick, D.M., Montgomery, R.L, Qi, X., Obad, S., Kauppinen, S., Hill, J.A., van Rooij, E. and Olson, E.N. (2010). Stress-dependant cardiac remodeling occurs in the absence of microRNA-21 in mice. *J Clin. Invest.*, 11, 3912-3916.
- Pedram, A., Razandi, M., Lubahn, D., Liu, J., Vannan, M. and Levin, E.R. (2008). Estrogen inhibits cardiac hypertrophy: role of estrogen receptor- β to inhibit calcineurin. *Endocrinology*, 149, 3361-3369.

- Posch, M.G., Perrot, A., Berger, F. and Özcelik, C. (2010). Molecular genetics of congenital atrial septal defects. *Clin. Res. in Cardiol.*, 99, 137-147.
- Potter, L.R., Yoder, A.R., Flora, D.R., Antos, L.K. and Dickey, D.M. (2009). Natriuretic peptides: their structures, receptors, physiologic functions and therapeutic applications. *cGMP: Generators, Effectors and Therapeutic Implications*, 341 Handbook of Experimental Pharmacology, Springer-Verlag Heidelberg.
- Prasad, S.V.N., Duan, Z., Gupta, M.K., Surampudi, V.S.K., Volinia, S., Calin, G.A., Liu, C.G., Kotwal, A., Moravec, C.S., Starling, R.C., Perez, D.M., Sen, S., Wu, Q., Plow, E.F., Croce, C.M. and Karnik, S. (2009). Unique microRNA profile in end-stage heart failure indicates alterations in specific cardiovascular signaling networks. *J. Biol. Chem.*, 284, 27487-27499.
- Prossnitz, E.R. and Barton, M. (2009). Signaling, physiological functions and clinical relevance of the G-protein coupled estrogen receptor GPER. *Prostaglandins Other Lipid Mediat.*, 89, 89-97.
- Prossnitz, E.R. and Maggiolini, M. (2009). Mechanisms of estrogen signaling via GPR30. *Mol. Cell Endocrinol.*, 308, 32-38.
- Rat Genome Sequencing Project Consortium. (2004). Genome sequence of the brown Norway rat yields Insights into mammalian evolution. *Nature*, 428, 493-520.
- Savoia, C., Volpe, M., Alonzo, A., Rossi, C and Rubattu, S. (2010). Natriuretic peptides and cardiovascular damage in the metabolic syndrome: molecular mechanisms and clinical implications. *Clin. Sci.*, 118, 231-240.
- Saxena, A. and Tabin, C.J. (2010). miRNA processing enzyme dicer is necessary for cardiac outflow tract alignment and chamber septation. *PNAS*, 107, 87-91.
- Sayed, D., Hong, C., Chen, I., Lypowy, J. and Abdellatif, M. (2007). MicroRNAs play an essential role in the development of cardiac hypertrophy. *Circ. Res.*, 100, 416-424.
- Shen, E., Diao, X., Wei, C., Wu, Z., Zhang, L. and Hu, B. (2010). MicroRNAs target gene and signaling pathway by bioinformatics analysis in the cardiac hypertrophy. *Biochem.Biophys. Res. Commun.*, 397, 380-385.
- Seixas Bello Moreira, A., Teixeira, M.T., Osso, F.S., Pereira, R.O., Silva-Junior, G.O., Garcia de Souza, E.P., Mandarim de Lacerda, C.A. and Sanchez Moura, A. (2009). Left ventricular hypertrophy induced by overnutrition early in life. *Nutr. Met. Cardiovas. Dis.*, 19, 805-810.
- Sucharov, C., Bristow, M.R. and Port, J.D. (2008). miRNA expression in the failing human heart: function correlates. *J. Mol. Cell Cardiol.*, 45, 185-192.

- Sumiyoshi, K., Kubota, S., Ohgawara, T., Kawata, K., Nishida, T., Shimo, T., Yamashiro, T. and Takigawa, M. (2010). Identification of miR-1 as a micro RNA that supports late-stage differentiation of growth cartilage cells. *Biochem. Biophys. Res. Commun.*, 402, 286-290.
- Suzuki, H.I. and Miyazono, K. (2010). Dynamics of microRNA biogenesis: crosstalk between p53 network and microRNA processing pathway. *J. Mol. Med.*, 88, 1085-1094.
- Tatsuguchi, M., Seok, H.Y., Callis, T.E., Thomson, J.M., Chen, J., Newman, M., Rojas, M., Hammond, S.M. and Wang, D. (2007). Expression of microRNAs is dynamically regulated during cardiomyocyte hypertrophy. *J. Mol. Cell Cardiol.*, 42, 1137-1141.
- Thum, T., Gross, C., Fiedler, J., Fischer, T., Kissler, S., Bussen, M., Galuppo, P., Just, S., Rottbauer, W., Frantz, S., Castoldi, M., Soutschek, J., Koteliansky, B., Rosenwald, A., Basson, M.A., Licht, J.D., Pena, J.T.R., Rouhanifard, S.H., Muckenthaler, M.U., Tuschl, T., Martin, G.L., Bauersachs, J. and Engelhardt, S. (2008). MicroRNA-21 contributes to myocardial disease by stimulating MAP kinase signaling in fibroblasts. *Nature*, 456, 980-986.
- Tsai, S., Lin, Y., Chu, S., Hsu, C. and Cheng, S. (2010). Interpretation and use of natriuretic peptides in non-congestive heart failure settings. *Yonsei Med. J.*, 51, 151-163.
- van Rooij, E., Liu, N. and Olson, E.N. (2008). MicroRNAs flex their muscles. *TIG*, 24, 159-166.
- van Rooij, E., Sutherland, L.B., Liu, N., Williams, A.H., McAnally, J., Gerard, R.D., Richardson, J.A. and Olson, E.N. (2006). A signature pattern of stress-responsive microRNAs that can evoke cardiac hypertrophy and heart failure. *PNAs*, 103, 18255-18260.
- van Rooij, E. and Olson, E.N. (2007). MicroRNAs: powerful new regulators of heart disease and provocative therapeutic targets. *J. Clin. Invest.*, 117, 2669-2376.
- Virgen-Ortiz, A., Marin, J.L., Elizalde, A., Castro, E., Stefani, E., Toro, L. and Muñiz, J. (2009). Passive mechanical properties of cardiac tissues in heart hypertrophy during pregnancy. *J. Physiol. Sci.*, 59, 391-396.
- Wang, J., Greene, S.B., Bonilla-Claudio, M., Tao, Y., Zhang, J., Bai, Y., Huang, Z., Black, B.L., Wang, F. and Martin, J.F. (2010). Bmp signaling regulates myocardial differentiation from cardiac progenitors through a microRNA-mediated mechanism. *Dev. Cell.*, 19, 903-912.

- Wang, J., Zhou, Z., Liao, X. and Zhang, T. (2009). Role of microRNAs in cardiac hypertrophy and heart failure. *IUBMB Life*, 61, 566-571.
- Yang, B., Lu, T. and Wang, Z. (2009). MicroRNAs and apoptosis: implications in the molecular therapy of human disease. *Clin. Exp. Pharmacol. Physiol.*, 36, 951-960.
- Yue, T., Gu, J., Wang, C., Reith, A.C., Lee, J.C., Mirabele, R.C., Kreutz, R., Wang, Y., Maleeff B., Parsons, A.A. and Ohlstein, E.H. (2000). Extracellular signal-related kinase plays an essential role in hypertrophic agonists, endothelin-1 and phenylephrine-induced cardiomyocyte hypertrophy. *Journal Biol. Chem.*, 275, 37895-37901.
- Zhang, C. (2008). MicroRNAs: role in cardiovascular biology and disease. *Clin. Sci.*, 114, 699-706.
- Zhang, X., Ashar, G., Helms, S.A. and Wei, J.Y. (2011). Regulation of cardiac microRNAs by serum response factor. *J. Biosoc. Sci.*, 18, 15-28.
- Zhao, Y. and Srivastava, D. (2007). A developmental view of microRNA function. *TIBS*, 32, 189-197.
- Zorio, E., Medina, P., Rueda, J., Millán, Arnau, M.A., Beneyto, M., Marín, F., Gimeno, J.R., Osca, J., Salvador, A., España and Estellés, A. (2009). Insights into the role of microRNAs in cardiac diseases: from biological signaling to therapeutic targets. *Cardio. Hem. Med. Chem.*, 7, 82-90.

Appendix A
IACUC Approval Letter



EASTERN KENTUCKY UNIVERSITY
Serving Kentuckians Since 1906

Graduate Education and Research
Division of Sponsored Programs
Institutional Animal Care and Use Committee

Jones 414, Coates CPO 20
521 Lancaster Avenue
Richmond, Kentucky 40475-3102
(859) 622-3636; Fax (859) 622-6610
<http://www.sponsoredprograms.eku.edu>

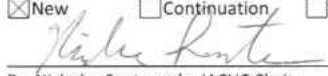
NOTIFICATION OF IACUC APPROVAL
OLAW Assurance Number A4575-01
Protocol Number: 04-2010

Principal Investigator: **Patricia Holden** Faculty Advisor: **Dr. Rebekah Waikel**

Project Title: **Characterization of miRNA Expression During Pregnancy**

Approval Date: **February 9, 2010** Expiration Date: **February 8, 2011**

Approval Type: New Continuation Amendment

Approval Signature: 
Dr. Nicholas Santangelo, IACUC Chair

This document confirms that the Institutional Animal Care and Use Committee (IACUC) has approved the above referenced activity as outlined in the application submitted for IACUC review with an immediate effective date.

Principal Investigator Responsibilities: It is the responsibility of the principal investigator to ensure that all investigators, staff, and students associated with this activity meet the training requirements for activities involving the use of animal subjects, follow the approved protocol, keep appropriate records, and comply with applicable University policies and state and federal regulations.

Adverse Events: Any adverse or unexpected events that occur in conjunction with this activity must be reported to the IACUC within ten calendar days of the occurrence. Immediate medical attention from a qualified physician must be arranged for any adverse events related to the health of humans involved in the activity. Immediate medical attention from a qualified veterinarian must be arranged for any adverse events related to the health of animals.

Records: Records related to this activity must be maintained for a minimum of three years following the completion of the activity and are subject to audit.

Changes to Approved Protocol: If changes to the approved protocol become necessary, a description of those changes must be submitted for IACUC review and approval prior to implementation. Changes include, but are not limited to, those related to personnel, procedures, types of animals, or quantities of animals for the activity.

Annual IACUC Continuing Review: This approval is valid for a period of not longer than one year. If the activity is to extend longer than one year, it is the responsibility of the principal investigator to submit an annual application for continuing review and receive approval prior to the anniversary date of the approval. Continuing reviews may be used to extend approval of the activity for up to three years from the original approval date, after which time a new application must be filed for IACUC review and approval.

Final Report: Within 30 days from the expiration of the activity, a final report must be filed with the IACUC.

Animal Care and Use Committee

Nicholas Santangelo, Chair, Biological Sciences	Kenneth Dickey, Attending Veterinarian	Linda Frost, Director, Honors Program
Don Llewellyn, Agriculture	Robert Mitchell, Psychology	Pradeep Bose, Student Health Services
Tim Weckman, Biological Sciences	Michael Judge, Community Representative	Harry Hebert, Community Representative
Jerry Pogatshnik, Institutional Official, AVP for Research	Gus Benson, Director, Sponsored Programs, ex-officio	

Appendix B

Dr. Rebekah Waikel's FastPrep RNA Extraction Protocol

Dr. Rebekah Waikel's FastPrep RNA Extraction Protocol

(Used for approximately 100mg of tissue or tissues w/ low RNA yield)

- 1) Add 1ml Trizol to the FastPrep tube.
- 2) Add 100-150mg tissue.
- 3) Homogenize sample using FastPrep instrument for 20 seconds @ speed setting of 6.0.

(May need to homogenize again if there are still pieces of tissue visible, cool on ice before doing so.)
- 4) Remove and centrifuge tube @12,000 x g for 5 minutes at 40C.
- 5) Transfer upper phase to new tube avoid matrix and cell debris.
- 6) Add 300µl of chloroform and vortex 10 seconds.
- 7) Incubate 5 minutes @ room temperature.
- 8) Centrifuge @ 12,000 x g for 5 minutes at 40C.
- 9) Transfer upper phase, avoiding white interface, to new tube.
- 10) Add 250µl High Salt solution, then 250µl isopropanol.
- 11) Invert tube and incubate for 20-30 minutes at room temperature.
- 12) Centrifuge @ 12,000 x g for 15 minutes at 40C.
- 13) Pour off supernatant making sure the pellet stays in the tube.
- 14) Wash pellet using 700µl 75% ethanol, pipette up and down a few times.
- 15) Remove as much ethanol as possible, wash again using 75% ethanol. Transfer pellet into fresh tube.
- 16) If pellet breaks into pieces centrifuge, remove ethanol.
- 17) Quick spin and remove as much ethanol as possible. (Use p10 to remove trace amounts of ethanol.)
- 18) Air dry pellet for 2-3 minutes.
- 19) Add appropriate amount of Rnase-free water to re-suspend the pellet.
- 20) Incubate samples @60°C for 10 minutes, if pellet is not re-suspended keep incubating for 10 minutes

until re-suspended.

21) Make a 1:10 dilution for each sample. Check the concentration as well as the 260/280 ratio on the nanodrop.

22) Make the correct dilutions and check the quality of each sample on the Agilent Bioanalyzer.

23) For long-term storage, precipitate RNA. Add 1/10 of total volume 3M NaAcetate, and then add 2.5x total volume. Store in -80°C .

Appendix C
Individual Cardiomyocyte Areas

Table 5. Individual cardiomyocyte areas measured in μm^2 . Below is the raw data for individual cardiomyocyte sizes measured for each rat sample for each group, Not Pregnant (NP), Pregnant (P), and Post Pregnant (PP).

NP										P			PP			
2007	4002	4004	4006	4007	4008	5004	6001	6010		4003	5001	6002	4001	6005	6006	6009
436.86	360.42	464.05	237.33	294.66	464.17	464.23	294.9	426.01		314.01	789.09	565.02	391.92	380.77	431.79	423.18
430.43	332.88	311.88	218.22	260.63	422.69	439.75	242.88	402.65		297.92	750.04	555.69	379.89	354.59	431.2	382.51
378.18	328.22	303.86	205.84	248.42	412.15	423.08	239.63	382.66		269.77	716.72	530.64	337.01	328.33	383.6	364.27
376.05	302.8	293.48	206.19	230.85	377.41	415.69	234.21	363.08		264.64	705.69	459.51	321.97	311.88	377.71	359.45
328.93	279.09	291.12	203.83	227.37	371.57	414.63	230.26	358.07		257.74	695.9	453.61	321.97	291.83	376.47	357.86
309.41	276.02	288.17	197.99	219.7	366.38	397.23	225.71	357.48		246.42	695.78	452.96	320.65	280.98	363.49	352.7
309.29	266.76	284.22	192.86	215.39	356.06	393.98	225.18	327.81		235.03	688.35	446.83	291.36	278.27	356.24	336.77
307.64	265.94	278.86	192.1	212.5	348.51	389.68	224.89	317.84		234.86	654.85	443.35	290.59	253.79	355.65	329.4
304.45	265	269.18	179.89	207.14	344.91	377.17	224.12	316.13		232.14	632.67	409.61	285.82	240.87	352.17	311.75
298.73	264.7	267.3	179.83	202.42	342.55	366.65	223.3	315.3		224.12	574.93	398.23	285.58	234.8	347.86	311.68
291.01	262.7	266.59	178.89	202.06	342.38	362.13	222.71	314.24		221.76	573.46	392.98	283.1	218.4	346.99	305.71
278.68	262.34	263.82	176.82	198.35	341.26	353.46	221.94	311.12		220.82	561.96	388.5	281.53	207.73	339.13	297.17
275.79	261.46	258.8	174.43	197.29	325.69	340.82	218.34	310.59		218.34	560.31	378.47	277.43	203.66	335.3	292.83
267.77	261.34	256.68	171.16	197.29	313.24	340.19	211.5	306.69		208.37	553.88	377.35	273.96	199.53	334.06	290.21
265.17	257.33	256.03	167.86	194.16	311.83	339.43	210.44	305.99		205.9	549.28	375.11	272.66	199.29	333.53	289.94
263.4	255.09	253.44	167.09	190.45	310.65	337.89	205.6	301.92		203.24	547.04	375.05	268.06	188.79	330.62	288.71
262.87	253.97	253.32	166.85	190.39	308.11	336.71	204.54	301.62		202.65	542.48	373.93	266.82	184.72	324.8	287.23
256.56	243.76	250.19	164.44	177.53	304.28	333.21	202.36	301.56		199.06	532.7	368.37	261.69	182.95	322.56	282.63
250.84	242.23	248.83	163.9	177	302.45	332.59	197.35	300.32		194.04	514.6	366.85	261.57	182.42	320.32	279.31
250.45	241.34	244.85	162.96	176.41	301.35	332.41	191.51	299.56		186.32	501.27	357.89	250.49	174.52	319.26	277.91
249.84	239.16	242.7	162.03	174.58	299.44	332.06	191.51	296.61		185.45	497.05	348.1	247.48	174.05	318.49	277.47
249.6	236.1	242.64	161.07	172.28	295.19	329.46	190.98	296.61		183.72	487.23	346.74	241.17	167.56	317.31	272.65
240.75	232.32	242.47	159.6	171.51	295.02	328.99	187.56	293.72		183.31	484.99	343.97	239.93	166.62	316.19	272.49
239.75	231.32	238.4	154.29	167.15	293.54	326.69	185.43	285.4		182.13	476.79	343.97	235.56	165.79	316.13	272.43
238.46	228.19	238.34	154.05	165.79	293.25	317.37	184.67	281.39		179.24	475.49	339.01	234.03	165.02	316.13	270.41
238.63	226.6	237.22	152.11	164.61	289.65	316.13	182.48	280.98		178	470.6	338.4	233.91	161.37	309.52	270.13
228.78	225.66	233.62	151.34	164.61	287.53	314.36	181.72	280.33		177.94	459.48	335.71	230.43	160.07	308.85	269.93
228.78	224.55	232.57	150.55	163.55	287.17	312.06	178.71	271.8		177.94	449.37	333.43	230.32	155.55	308.11	266.84
228.02	223.89	230.32	150.52	162.08	287.11	311.94	177.82	270.54		169.27	439.63	313.54	226.48	149.69	306.4	266.38
226.13	222.59	227.31	150.22	159.89	286.4	308.82	175.52	269.42		174.11	443.82	322.38	228.19	135.12	304.63	261.31
225.89	220.23	223.06	147.68	158.18	285.28	307.28	172.52	269.24		171.75	442.82	320.61	227.66	119.02	303.67	260.75
223.95	218.11	222.65	146.62	157.83	285.23	306.87	167.74	265.88		171.45	442.7	316.54	226.89	115.13	302.27	255.03
222.82	216.75	222.47	145.8	157.24	282.93	305.51	166.68	264.17		170.33	441.17	315.54	226.6	109.41	300.28	250.72
221.59	215.22	222.47	145.74	155.82	281.39	305.46	164.67	262.05		166.26	438.15	307.87	226.48	102.54	299.09	244.24
219.82	213.92	221.65	144.62	155.65	281.39	299.2	162.37	261.81		166.26	438.15	307.87	225.3	352.3	299.09	245.84
214.21	212.95	221.29	143.5	151.87	281.27	298.85	161.96	260.39		165.67	415.33	306.81	222.29	332.88	298.67	243.31
213.62	212.68	219.85	142.83	150.93	280.62	297.09	161.84	257.68		164.61	413.68	305.93	219.4	333.11	291.42	230.58
208.08	212.5	219.7	141.9	150.75	274.96	297.02	160.96	256.38		162.25	408.09	304.16	218.67	321.89	290.24	230.24
207.84	212.39	217.87	141.73	149.87	274.67	296.48	160.07	256.03		160.13	405.13	300.38	218.4	287.7	284.64	230.02
205.84	211.09	217.28	140.25	149.63	273.9	294.64	158.24	255.09		159.42	404.6	295.18	217.96	280.2	281.1	228.9
204.95	210.14	215.04	139.43	148.98	271.72	291.65	156.94	254.73		158.54	403.66	294.96	217.99	270.78	274.67	222
200.83	207.31	212.39	138.66	148.81	270.95	291.12	156.53	254.32		157.95	393.98	294.01	215.98	265.23	273.84	219.57
200.59	207.14	211.44	138.6	148.45	270.66	286.35	156.18	254.03		156.24	391.09	293.25	214.92	249.66	273.37	217.07
200.59	206.66	211.21	138.43	148.91	268.96	284.28	155.82	253.61		155	390.27	291.14	214.45	247.21	271.37	208.49
198.64	206.55	210.44	134.89	143.78	267.71	281.63	155.29	252.67		154.7	373.22	288.88	212.92	238.2	271.37	207.4
197.76	205.65	209.97	133.23	143.03	262.58	278.44	154.29	249.48		152.58	368.86	282.93	212.15	236.29	268.77	206.78
192.69	204.6	209.2	131.47	142.97	261.81	281.43	152.64	246.65		152.17	366.28	281.98	211.32	218.45	268.06	206.33
187.14	204.31	207.73	129.64	142.44	261.4	270.92	152.34	245.83		147.1	360.48	281.92	207.02	217.27	264.29	205.78
185.9	203.95	205.19	129.64	140.49	260.81	270.24	149.34	243.88		145.15	357.93	281.63	206.55	208.2	261.93	202.49
185.61	203.83	203.54	128.75	140.08	260.04	265.7	149.1	243.29		142.14	356	281.51	203.6	207.7	261.81	202.12
185.08	202.71	203.01	128.27	139.78	258.92	264.89	148.92	241.29		141.43	354.29	281.05	202.71	206.1	252.37	201.36
184.43	200.18	203.01	127.75	138.07	255.26	261.1	148.45	240.81		140.9	353.85	278.59	200.77	202.09	252.2	200.18
183.77	198.35	202.59	127.28	136.12	254.32	257.8	148.16	238.04		139.96	352.99	276.26	200.12	179.17	251.96	194.15
182.84	194.57	201.65	127.09	132.65	253.61	256.27	147.39	233.44		138.19	350.34	269.65	198.23	171.84	251.55	192.79
177.35	194.04	199.47	125.92	130.88	253.14	254.85	146.68	232.85		137.89	350.27	269.6	196.67	167.49	251.49	189.15
174.76	190.98	199.35	125.27	129.81	249.31	247.07	146.21	232.79		137.13	346.39	269.6	195.16	162.84	250.84	187.25
173.34	190.62	199.17	125.15	128.93	248.13	246.77	145.03	232.26		135	338.6	266.35	192.39	380.24	250.25	186.66
173.22	189.56	198.35	125.1	128.16	247.6	245.06	144.68	230.96		134.3	337.65	259.57	189.32	345.97	247.48	186.01
172.87	188.91	197.82	124.45	127.99	247.54	242.32	144.44	230.67		130.17	333.97	253.61	189.09	305.81	246.53	182.62
167.95	188.91	196.34	124.17	127.69	246.56	241.26	141.61	230.26		127.93	333.88	252.43	188.91	288.88	243.76	182.25
166.74	188.03	195.93	123.49	127.51	243.11	241.09	141.2	226.88		127.08	332.85	251.9	188.85	262.4	243.64	180.74
164.91	187.44	195.81	118.46	126.33	241.58	240.52	140.49	225.48		127.87	327.51	251.9	187.66	254.2	241.29	179.22
163.08	187.2	194.4	117.91	126.16	238.16	240.22	138.9	224.95		127.81	325.74	250.84	187.84	244.94	240.93	175.57
161.49	185.43	185.15	115.95	125.92	234.74	238.28	137.95	223.47		124.45	324.8	247.64	181.72	234.5	235.74	171.82
160.13	181.42	187.44	115.59	125.8	230.26	237.04	137.6	222.47		123.03	320.35	247.54	181.07	224.77	235.62	168.71
159.83	179.59	187.08	115.19	125.63	229.14	236.04	137.25	222.12		120.97						